December 14, 2017

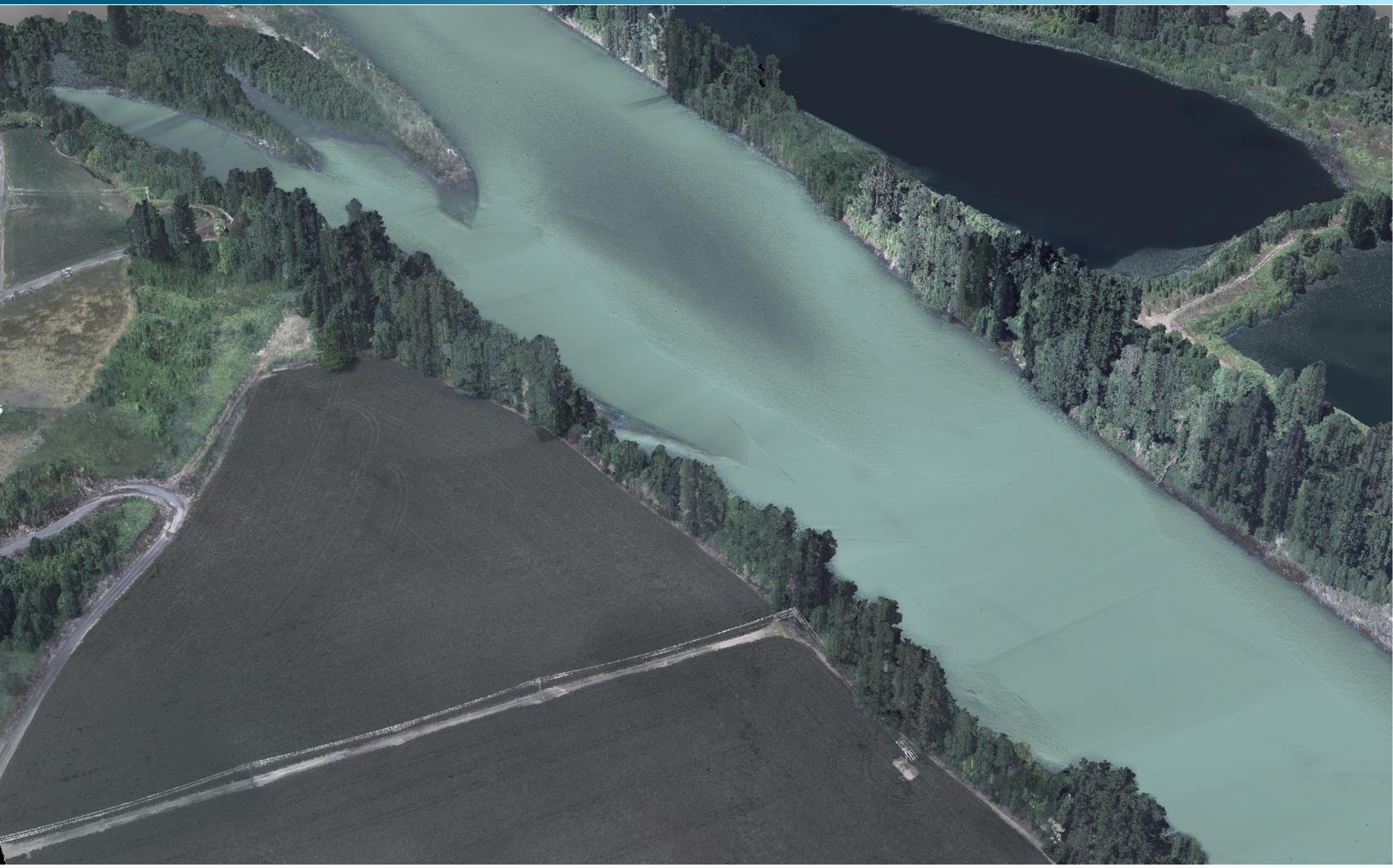

Willamette River, Oregon Topobathymetric LiDAR

Technical Data Report, Contract # W91278-16-D-0112/0001

US Army Corps of Engineers

Chris Macon
USACE Mobile District JALBTCX
7225 Stennis Airport Rd, Suite 100
Kiln, MS 39556

QSI Corvallis
517 SW 2nd St., Suite 400
Corvallis, OR 97333
PH: 541-752-1204

Table of Contents

Cover Photo: A view looking south over the Willamette River in Oregon. The image was created from the LiDAR bare earth model overlaid with the above ground point cloud and colored by ortho-imagery.

INTRODUCTION

This photo taken by QSI acquisition staff shows a view of the Willamette River landscape within the Willamette River project area

In September 2016, Quantum Spatial (QSI) was contracted by The United States Army Corps of Engineers Mobile District (USACE) to collect topobathymetric Light Detection and Ranging (LiDAR) data in the spring of 2017 for a portion of the Willamette River in Oregon. The Willamette River project area of interest (AOI) stretches from Springfield, Oregon to Oregon City, Oregon, a total area of 108,963 acres. Data were collected to aid USACE in studying anadromous fish passage and floodplain management. The high resolution data will help in the detailed classification and quantification of aquatic habitat, flood modeling, and water quality monitoring.

This report accompanies the full delivery of topobathymetric LiDAR data and co-acquired photography, superseding the previously delivered report. This report documents contract specifications, data acquisition procedures, processing methods, and analysis of the final dataset, including LiDAR accuracy and density. Acquisition dates and acreage are shown in Table 1, a complete list of contracted deliverables provided to USACE is shown in Table 2, and the project extent is shown in Figure 1.

Table 1: Acquisition dates, acreage, and data types collected on the Willamette River, Oregon Delivery

Project Site	Contracted Acres	Buffered Acres	Acquisition Dates	Data Type
Willamette River, Oregon	96,146	108,963	05/28/17, 05/29/17, 06/02/17, 06/05/17 – 06/07/17, 06/14/17, 06/17/17 – 06/20/17, 06/25/17, 06/29/17	Topobathymetric LiDAR RGB Imagery

Deliverable Products

Table 2: Products delivered to USACE for the Willamette River Topobathymetric LiDAR Delivery

Willamette River, Oregon Topobathymetric LiDAR Products Projection: UTM Zone 10 North Horizontal Datum: NAD83 (2011) Vertical Datum: NAVD88 (GEOID 12B) Units: Meters	
Topobathymetric LiDAR	
Points	LAS v 1.4 • All Classified Returns • Unclassified Flightline Swaths
Rasters	1.0 Meter ESRI Grids • Topobathymetric Bare Earth Digital Elevation Model (DEM), Interpolated and Clipped[1] • Highest Hit Digital Surface Model (DSM) • Ground and Bathymetric Bottom Classified Density Raster • First Return Density Raster 0.5 Meter GeoTiffs • Intensity Images
Vectors	Shapefiles (*.shp) • Contracted and Buffered Project Boundaries • LiDAR and Digital Imagery Tile Index • Raster Tile Index • Bathymetric Coverage Shape • Water's Edge Breaklines • Low Confidence Polygon • Smoothed Best Estimate Trajectory (SBETs) Comma Delimited ASCII Files (*.csv) • Smoothed Best Estimate Trajectory (SBETs)
Digital Imagery	10cm True Color Imagery • 500 x 500 m tiles (*.tif) • AOI Mosaic (*.sid)
Reporting	FGDC Compliant Metadata (*.xml) • Project-wide Metadata and Individual File *.xmls Supplemental Information and Datasheets • QSI airborne collection field log • QSI ground control field log • Ground control monument photos • NGS Control Sheets

[1] *Topobathymetric bare earth model clipped using a shaped derived from areas that lacked topobathymetric ground returns (see Topobathymetric DEMs, page 20*)

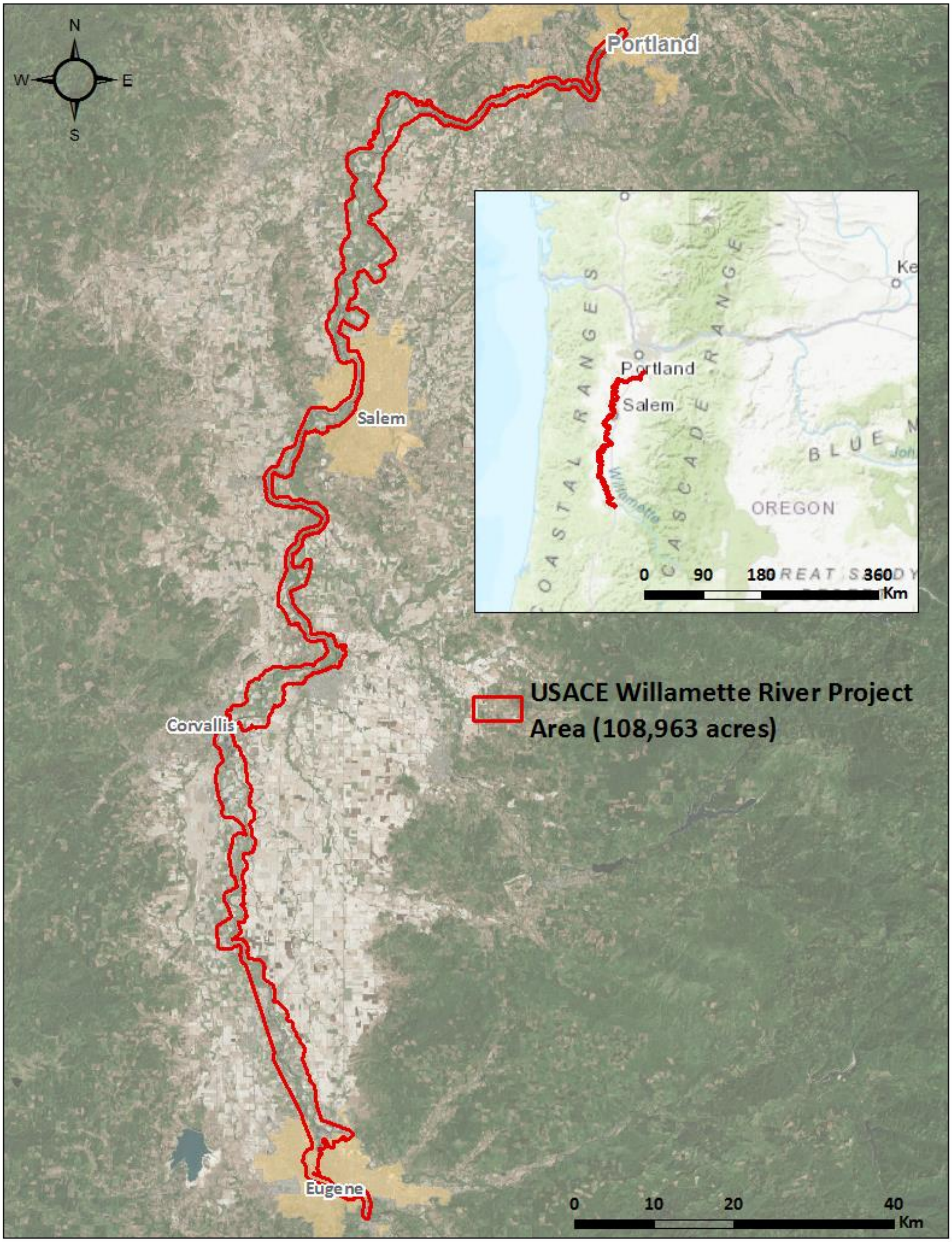

Figure 1: Location map of the Willamette River Topobathymetric LiDAR site

QSI's secchi depth collection location at the Oregon State University Rowing Dock in Corvallis, Oregon

Sensor Selection: the Riegl VQ-880-G

The Riegl VQ-880-G was selected as the hydrographic airborne laser scanner for the Willamette River Topobathymetric LiDAR project based on fulfillment of several considerations deemed necessary for effective mapping of the project site. A higher repetition pulse rate (up to 550 kHz), higher scanning speed, small laser footprint, and wide field of view allow for seamless collection of high resolution data of both topographic and bathymetric surfaces. A short laser pulse length allows for discrimination of underwater surface expression in shallow water, critical to shallow and dynamic environments such as the Willamette River. The Riegl VQ-880-G contains an integrated NIR laser (λ=1064 nm) that aids in water surface modeling. Sensor specifications and settings for the Willamette River acquisition are displayed in Table 3.

Planning

In preparation for data collection, QSI reviewed the project area and developed a specialized flight plan to ensure complete coverage of the Willamette River Topobathymetric LiDAR study area at the target point density of ≥8.0 points/m^2. Acquisition parameters including orientation relative to terrain, flight altitude, pulse rate, scan angle, and ground speed were adapted to optimize flight paths and flight times while meeting all contract specifications.

Factors such as satellite constellation availability and weather windows must be considered during the planning stage. Any weather hazards or conditions affecting the flights were continuously monitored due to their potential impact on the daily success of airborne and ground operations. Many logistical considerations including private property access, potential air space restrictions, and channel flow rates were reviewed (Figure 2 through Figure 5). Additionally, QSI actively monitored the water clarity of the Willamette River by taking daily secchi depth and turbidity readings from January through the end of acquisition in June to ensure that the data was acquired during optimal water clarity conditions (Figure 6 through Figure 8).

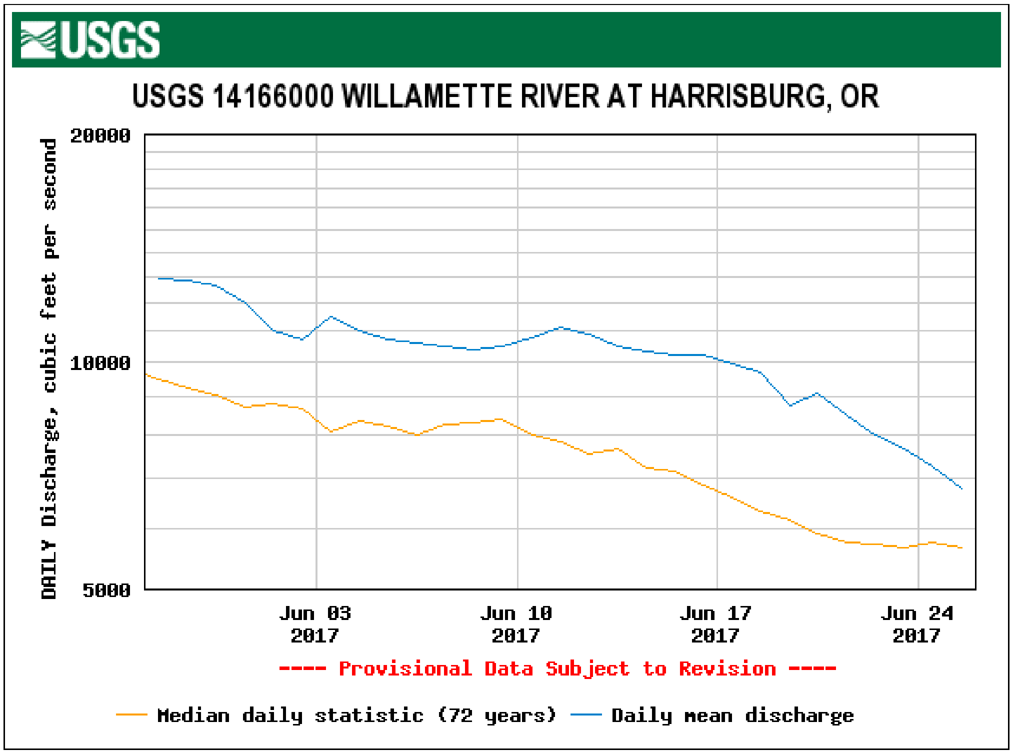

Figure 2: USGS Station 14166000 flow rates along the Willamette River, at Harrisburg, Oregon during the time of LiDAR acquisition.

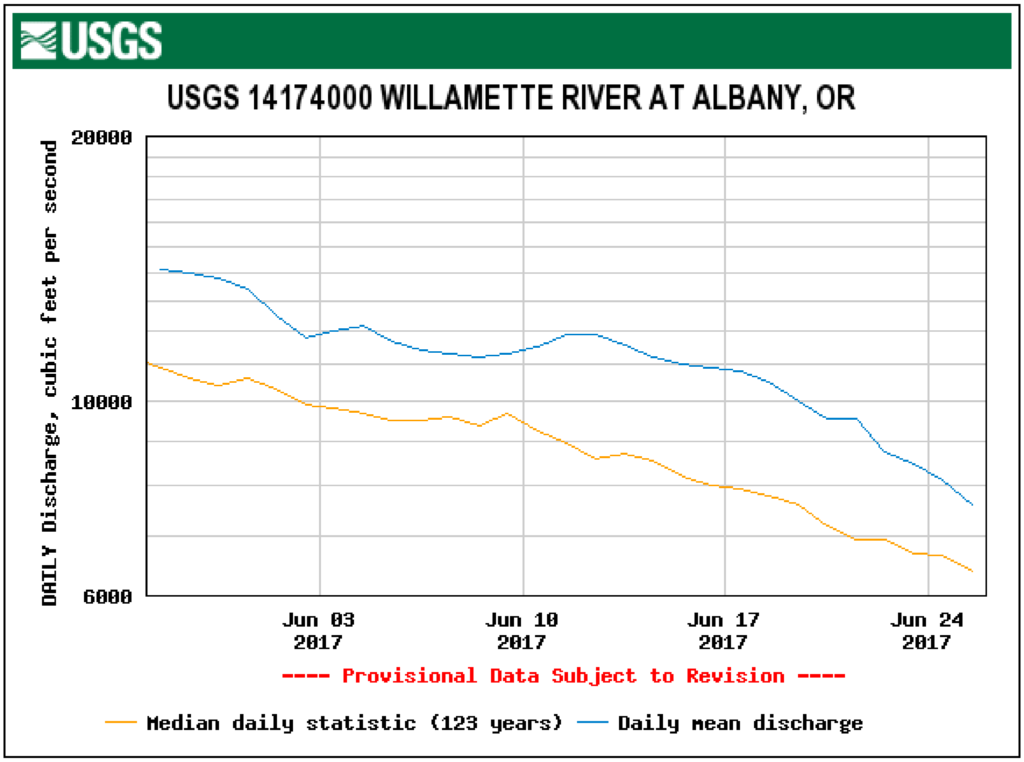

Figure 3: USGS Station 14174000 flow rates along the Willamette River, at Albany, Oregon during the time of LiDAR acquisition.

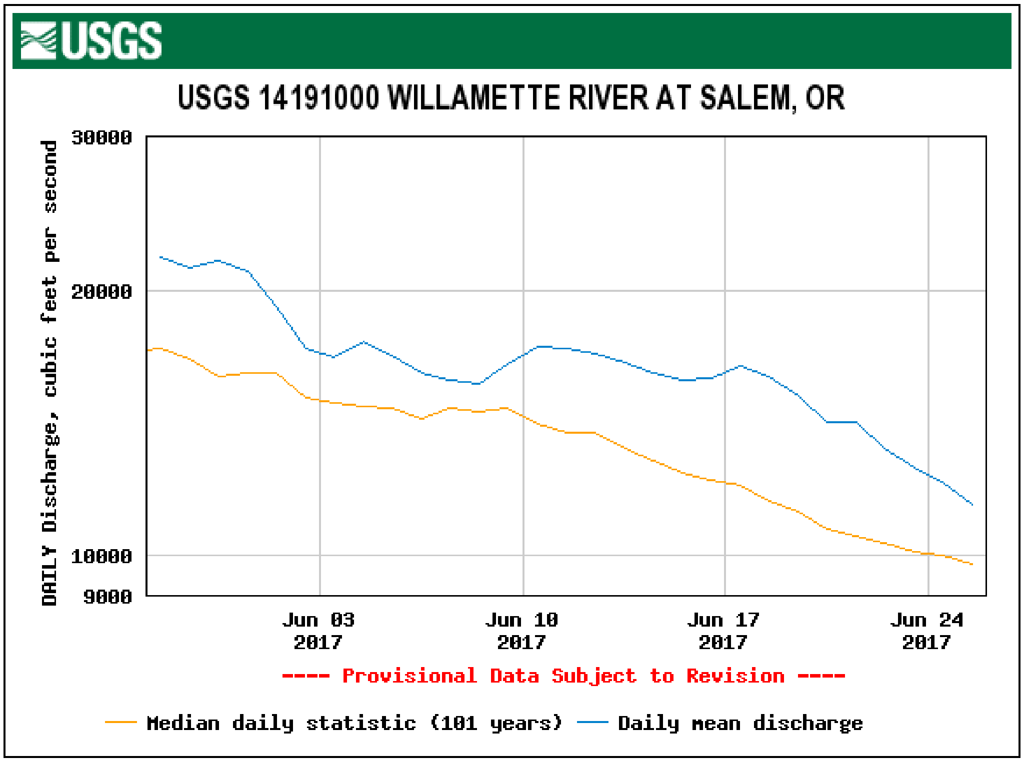

Figure 4: USGS Station 14174000 flow rates along the Willamette River, at Salem, Oregon during the time of LiDAR acquisition.

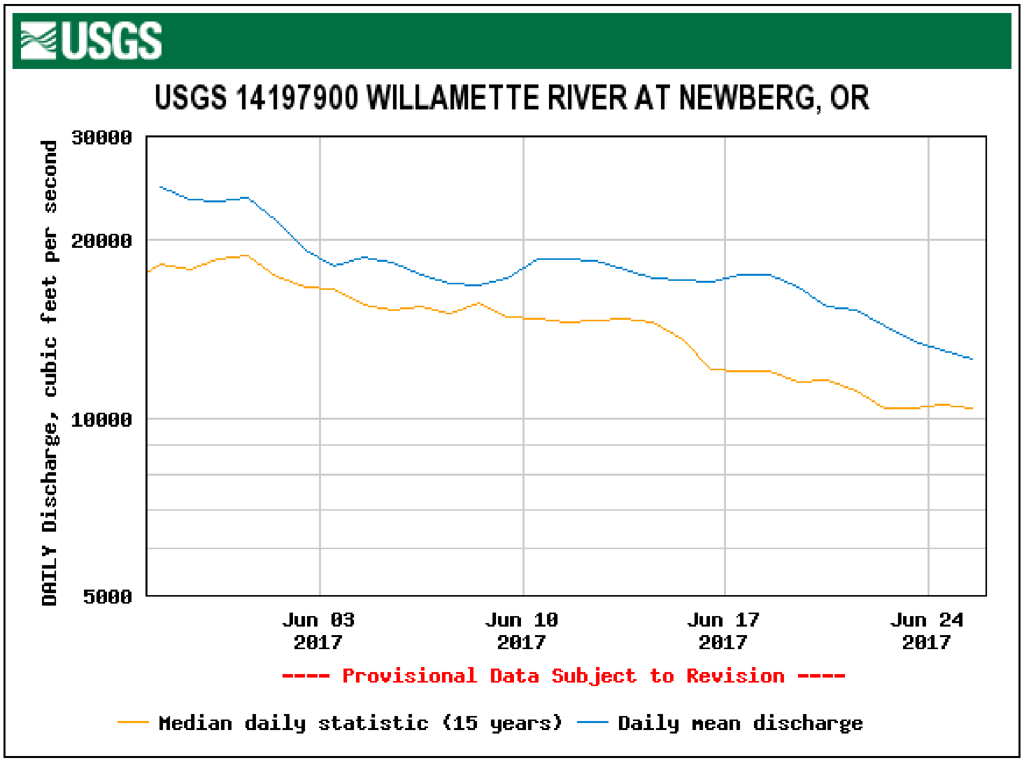

Figure 5: USGS Station 14174000 flow rates along the Willamette River, at Newberg, Oregon during the time of LiDAR acquisition.

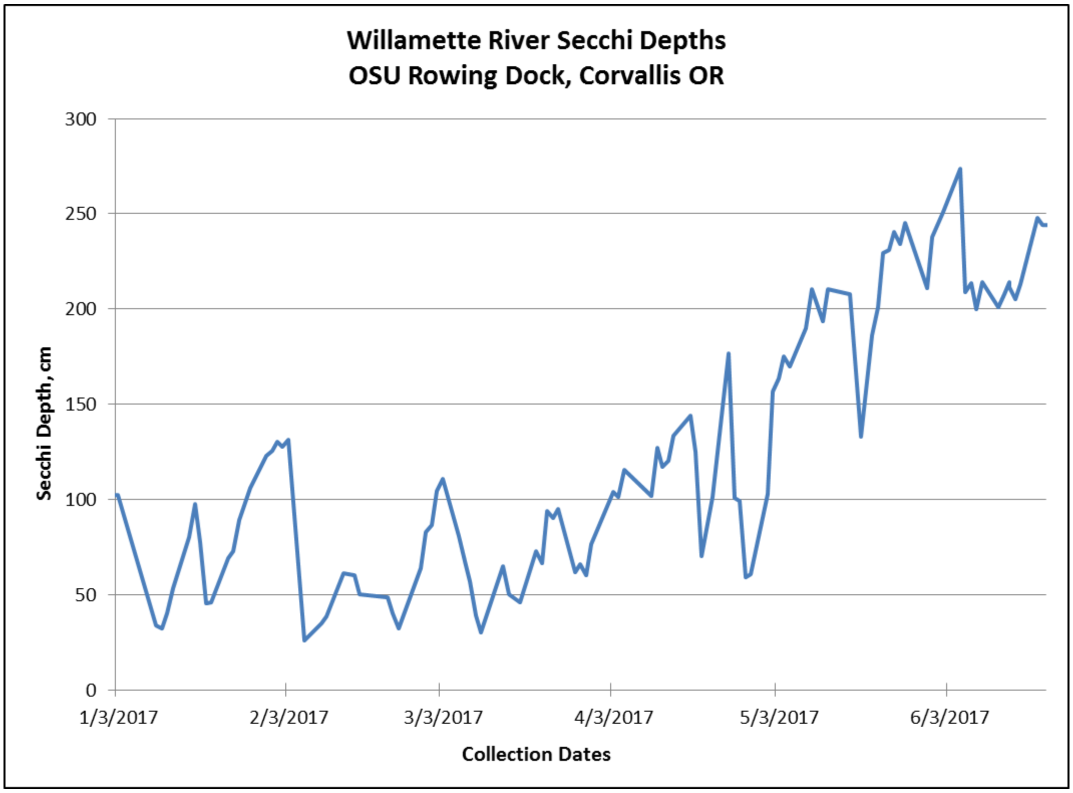

Figure 6: Willamette River Secchi Depths, at Corvallis, Oregon before and during the time of LiDAR acquisition.

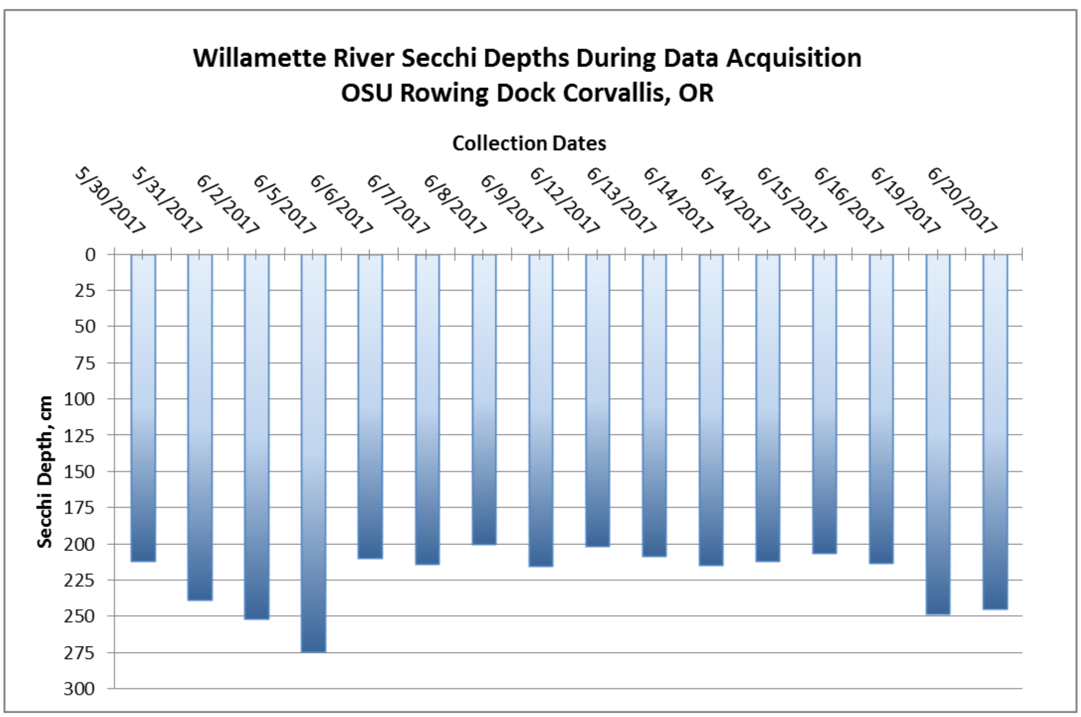

Figure 7: Willamette River secchi depths at Corvallis, Oregon during the data acquisition.

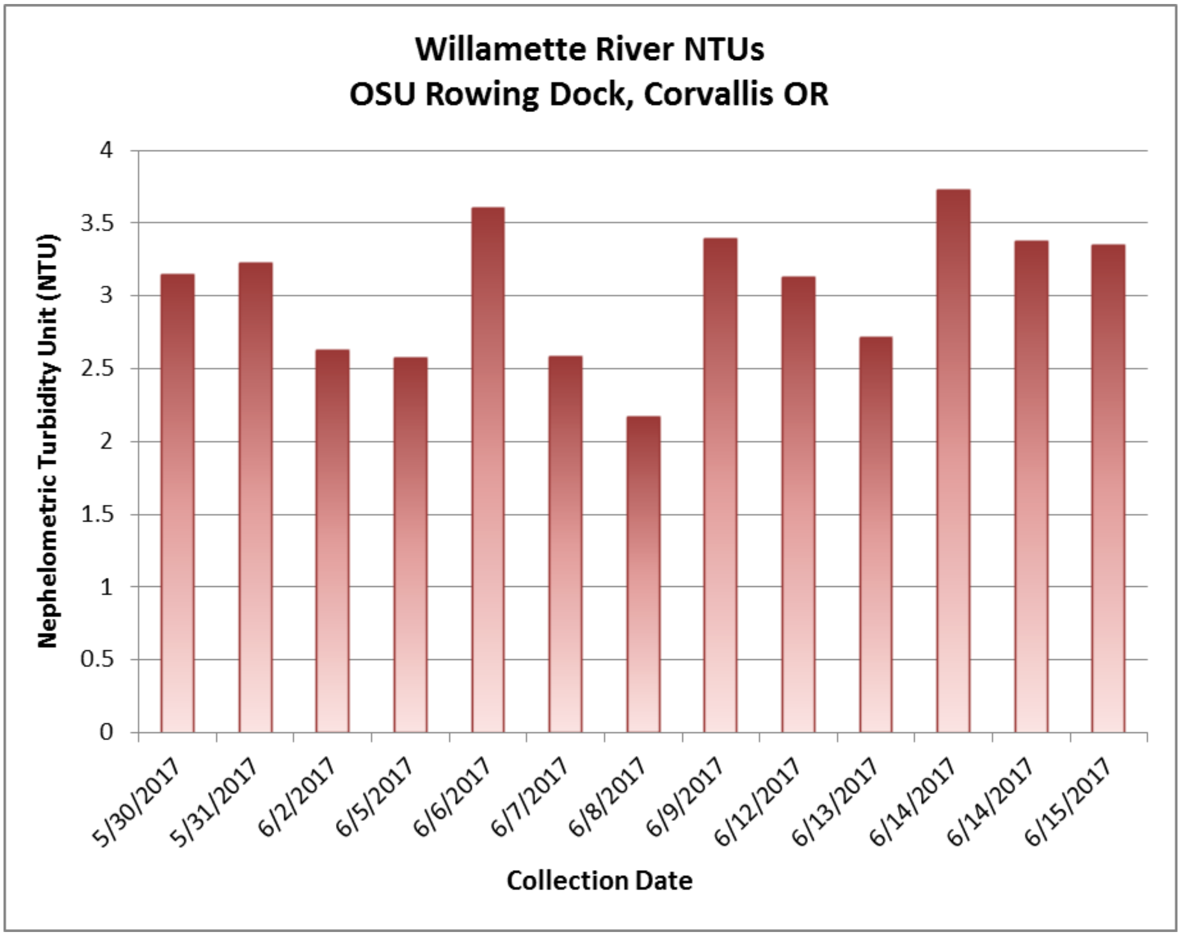

Figure 8: Willamette River Nephelometric Turbidity Units (NTUs) at Corvallis, Oregon during the data acquisition.

These photos taken by QSI acquisition staff display water clarity conditions at two locations within the Willamette River project area during the time of LiDAR acquisition.

Airborne Survey

LiDAR

The LiDAR survey was accomplished using a Riegl VQ-880-G green laser system mounted in a Cessna U206F. The Riegl VQ-880-G uses a green wavelength (ʎ=532 nm) laser that is capable of collecting high resolution vegetation and topography data, as well as penetrating the water surface with minimal spectral absorption by water. The recorded waveform enables range measurements for all discernible targets for a given pulse. The typical number of returns digitized from a single pulse range from 1 to 7 for the Willamette River Topobathymetric LiDAR project area. It is not uncommon for some types of surfaces (e.g., dense vegetation or water) to return fewer pulses to the LiDAR sensor than the laser originally emitted. The discrepancy between first return and overall delivered density will vary depending on terrain, land cover, and the prevalence of water bodies. All discernible laser returns were processed for the output dataset. Table 3 summarizes the settings used to yield an average pulse density of ≥8 pulses/m^2 over the Willamette River Topobathymetric LiDAR project area.

Table 3: LiDAR specifications and survey settings

LiDAR Survey Settings & Specifications	
Acquisition Dates	05/28/17, 05/29/17, 06/02/17, 06/05/17 – 06/07/17, 06/14/17, 06/17/17 – 06/20/17, 06/25/17, 06/29/17
Aircraft Used	Cessna U206F
Sensor	Riegl
Laser	VQ-880-G
Maximum Returns	Unlimited
Resolution/Density	Average 8 pulses/m^2
Nominal Pulse Spacing	0.35 m
Survey Altitude (AGL)	400 m
Survey speed	120 knots
Field of View	40^o
Mirror Scan Rate	80 lines per second
Target Pulse Rate	245 kHz
Pulse Length	1.3 ns
Laser Pulse Footprint Diameter	40 cm
Central Wavelength	532 nm
Pulse Mode	Multi Pulse in Air (MPIA)
Beam Divergence	0.7 mrad
Swath Width	291 m
Swath Overlap	55 %
GPS Baselines	≤13 nm
GPS PDOP	≤3.0
GPS Satellite Constellation	≥6
Intensity	16-bit
Accuracy	$RMSE_Z$ ≤ 15 cm

All areas were surveyed with an opposing flight line side-lap of ≥50% (≥100% overlap) in order to reduce laser shadowing and increase surface laser painting. To accurately solve for laser point position (geographic coordinates x, y and z), the positional coordinates of the airborne sensor and the attitude of the aircraft were recorded continuously throughout the LiDAR data collection mission. Position of the aircraft was measured twice per second (2 Hz) by an onboard differential GPS unit, and aircraft attitude was measured 200 times per second (200 Hz) as pitch, roll and yaw (heading) from an onboard inertial measurement unit (IMU). To allow for post-processing correction and calibration, aircraft and sensor position and attitude data are indexed by GPS time.

Digital Imagery

Aerial imagery was co-acquired with the topobathymetric LiDAR data using a Prosilica GT 6600 28.8 megapixel digital camera (Table 4). For the Willamette River Topobathymetric LiDAR site, images were collected in three spectral bands (red, green, and blue). Flight planning was optimized for LiDAR collection thus sun angle and image frame overlap were not always ideal for photography; in a few rare circumstances data voids exist. At 400 meters flying height the camera is able to resolve imagery at a 10 cm resolution. Orthophoto specifications particular to the Willamette River project area are shown in Table 5.

Table 4: Camera manufacturer's specifications

Prosilica GT 6600 Specifications	
Focal Length	51 mm
Data Format	RGB
RCD Pixel Size	5.5 µm
Image Size	6,576 x 4,384 pixels
Frame Rate	3 seconds
FOV	40° x 27°

Table 5: Project-specific orthophoto specifications

Digital Orthophotography Specifications	
Equipment	Prosilica GT 6600
Spectral Bands	Red, Green, Blue
Resolution	10 cm pixel size
Survey Altitude (AGL)	400 meters
GPS Baselines	≤25 nm
GPS PDOP	≤3.0
GPS Satellite Constellation	≥6
Image	8-bit GeoTiff

Ground Control

Ground control surveys, including monumentation and ground survey points (GSPs), were conducted to support the airborne acquisition. Ground control data were used to geospatially correct the aircraft positional coordinate data and to perform quality assurance checks on final LiDAR data.

Existing NGS Monument

QSI-Established Monument

Monumentation

The spatial configuration of ground survey monuments provided redundant control within 13 nautical miles of the mission areas for LiDAR flights. Monuments were also used for collection of ground survey points using real time kinematic (RTK), post processed kinematic (PPK), and fast static (FS) survey techniques.

Monument locations were selected with consideration for satellite visibility, field crew safety, and optimal location for GSP coverage. QSI utilized six existing NGS monuments, six Trimble VRS-Now (TVRSN) permanent base stations, one Oregon Real-time GNSS Network (ORGN) station, two temporary survey nails, and four newly-established monuments for the Willamette River Topobathymetric LiDAR project (Table 6, Figure 10). New monumentation was set using 5/8" x 30" rebar topped with stamped 2 ½ " aluminum caps. QSI's professional land surveyor, Evon Silvia (ORPLS#81104) oversaw and certified the establishment of all monuments.

Table 6: Base stations utilized for the Willamette River Topobathymetric LiDAR acquisition. Coordinates are on the NAD83 (2011) datum, epoch 2010.00

Base Station ID	Network	Latitude	Longitude	Ellipsoid (meters)
DE5625	NGS Mark	44° 59' 40.62197"	-123° 06' 59.54832"	41.729
DE5640	NGS Mark	44° 44' 16.74277"	-123° 10' 52.50637"	40.854
OBEC	TVRSN	44° 03' 57.45967"	-123° 05' 53.27938"	112.201
ORCO	TVRSN	44° 33' 08.49678"	-123° 16' 06.84186"	56.194
ORDA	TVRSN	44° 55' 08.66755"	-123° 19' 40.16392"	95.806
ORMC	TVRSN	45° 13' 07.83450"	-123° 10' 02.41670"	34.849
ORSA	TVRSN	44° 53' 59.23909"	-123° 00' 30.84151"	55.270
ORTI	TVRSN	45° 24' 13.39500"	-122° 45' 28.12098"	35.350
P406	ORGN	45° 11' 25.32562"	-123° 09' 08.06499"	26.652
QE1502	NGS Mark	44° 11' 41.44022"	-123° 12' 11.23471"	79.772
QE1579	NGS Mark	44° 38' 23.26469"	-123° 09' 22.19394"	43.621
QE2232	NGS Mark	44° 09' 19.62555"	-123° 09' 19.65460"	86.510

Base Station ID	Network	Latitude	Longitude	Ellipsoid (meters)
RD1695	NGS Mark*	45° 03' 26.87106"	-123° 06' 15.53110"	129.161
WILLYBATH_01	QSI Mark	44° 31' 10.92253"	-123° 15' 04.67170"	44.920
WILLYBATH_02	QSI Mark	44° 23' 22.60510"	-123° 15' 01.02230"	56.241
WILLYBATHY_03	QSI Mark	45° 16' 28.61611"	-122° 46' 09.61046"	34.131
WILLYBATHY_04	QSI Mark	45° 17' 48.27407"	-122° 47' 54.39356"	33.057
WILLYBATH_RTK_01	Temp QSI Mark	44° 02' 04.04780"	-123° 01' 37.23025"	113.269
WILLYBATH_RTK_02	Temp QSI Mark	44° 06' 55.71585"	-123° 07' 01.03469"	93.765

*Mark RD1695 is likely an undocumented RESET of the original NGS mark. QSI recovered the mark in approximately the published position, but it was an orange plastic cap and not a bronze cap set in concrete as published in the NGS datasheet.

To correct the continuously recorded onboard measurements of the aircraft position, QSI concurrently conducted multiple static Global Navigation Satellite System (GNSS) ground surveys (1 Hz recording frequency) over each monument. During post-processing, the static GPS data were triangulated with nearby Continuously Operating Reference Stations (CORS) using the Online Positioning User Service (OPUS[2]) for precise positioning. Multiple independent sessions over the same monument were processed to confirm antenna height measurements and to refine position accuracy.

Monuments were established according to the national standard for geodetic control networks, as specified in the Federal Geographic Data Committee (FGDC) Geospatial Positioning Accuracy Standards for geodetic networks.[3] This standard provides guidelines for classification of monument quality at the 95% confidence interval as a basis for comparing the quality of one control network to another. The monument rating for this project is shown in Table 7.

Table 7: Federal Geographic Data Committee monument rating for network accuracy

Direction	Rating
1.96 * St Dev $_{NE}$:	0.020 m
1.96 * St Dev $_{z}$:	0.020 m

For the Willamette River Topobathymetric LiDAR LiDAR project, the monument coordinates contributed no more than 2.8 cm of positional error to the geolocation of the final ground survey points and LiDAR, with 95% confidence.

[2] OPUS is a free service provided by the National Geodetic Survey to process corrected monument positions. http://www.ngs.noaa.gov/OPUS/.

[3] Federal Geographic Data Committee, Geospatial Positioning Accuracy Standards (FGDC-STD-007.2-1998). Part 2: Standards for Geodetic Networks, Table 2.1, page 2-3. http://www.fgdc.gov/standards/projects/FGDC-standards-projects/accuracy/part2/chapter2

Ground Survey Points (GSPs)

Ground survey points were collected using real time kinematic (RTK), post-processed kinematic (PPK), and fast-static (FS) survey techniques. A Trimble R7 base unit was positioned at a nearby monument to broadcast a kinematic correction to a roving Trimble R8 GNSS receiver. All GSP measurements were made during periods with a Position Dilution of Precision (PDOP) of ≤ 3.0 with at least six satellites in view of the stationary and roving receivers. When collecting RTK and PPK data, the rover records data while stationary for five seconds, then calculates the pseudorange position using at least three one-second epochs. FS surveys record observations for up to fifteen minutes on each GSP in order to support longer baselines for post-processing. Relative errors for any GSP position must be less than 1.5 cm horizontal and 2.0 cm vertical in order to be accepted. See Table 8 for QSI Trimble unit specifications.

GSPs were collected in areas where good satellite visibility was achieved on paved roads and other hard surfaces such as gravel or packed dirt roads. GSP measurements were not taken on highly reflective surfaces such as center line stripes or lane markings on roads due to the increased noise seen in the laser returns over these surfaces. GSPs were collected within as many flightlines as possible; however, the distribution of GSPs depended on ground access constraints and monument locations and may not be equitably distributed throughout the study area (Figure 10).

Table 8: Trimble equipment identification

Receiver Model	Antenna	OPUS Antenna ID	Use
Trimble R7 GNSS	Zephyr GNSS Geodetic Model 2 RoHS	TRM57971.00	Static
Trimble R8	Integrated Antenna R8 Model 2	TRM_R8_GNSS	Rover

Camera Boresight

In order to directly georeference imagery from the airborne GPS (ABGPS), a boresight flight was conducted over Corvallis, Oregon on May 29th, 2017. Using post-processed aircraft trajectory data, camera calibration information, ground control, and auto-generated tie-points, boresight misalignment angles were computed for the Riegl camera and applied to subsequent data acquisition missions.

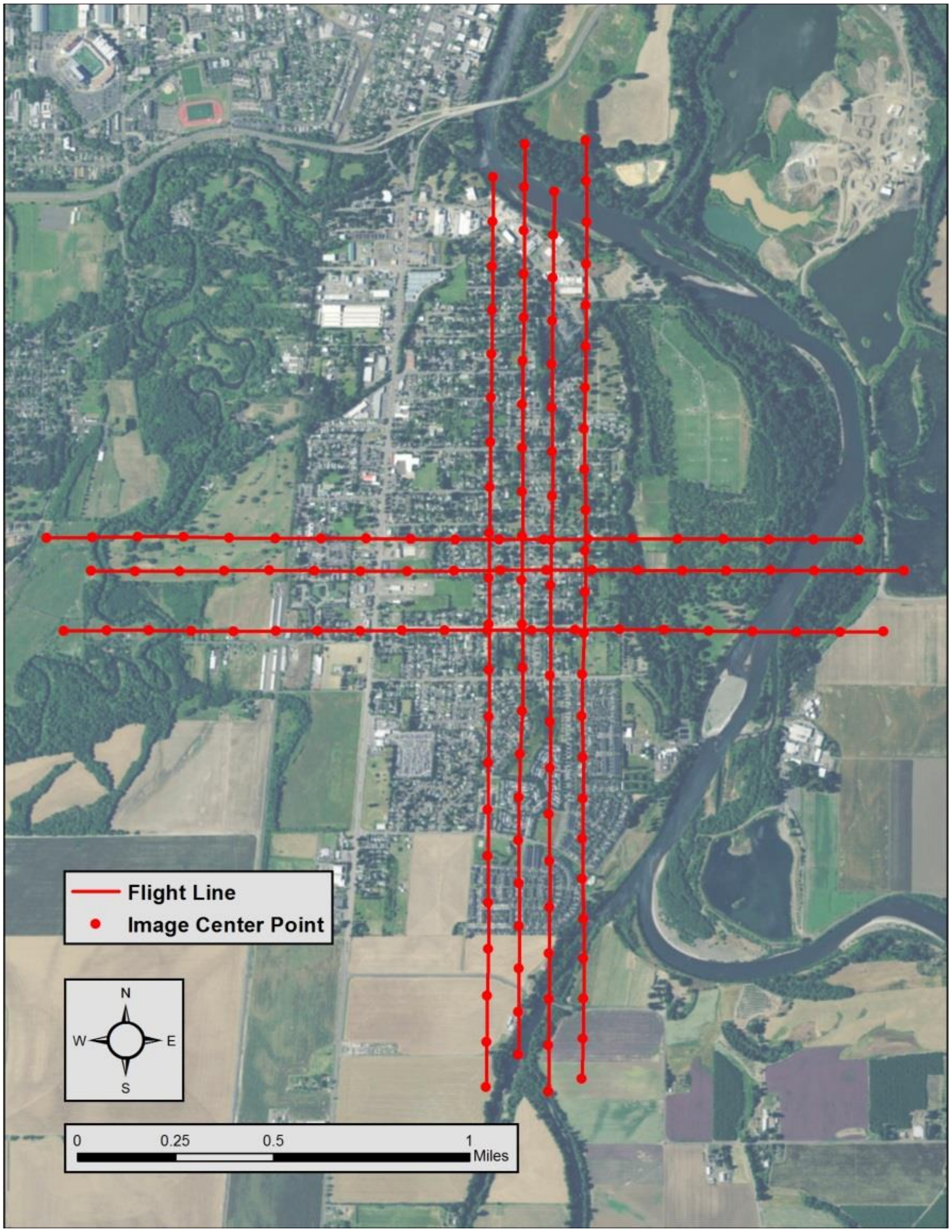

Figure 9: Boresight flight plan over Corvallis, Oregon

Land Cover Class

In addition to ground survey points, land cover class check points were collected throughout the study area to evaluate vertical accuracy. Vertical accuracy statistics were calculated for all land cover types to assess confidence in the LiDAR derived ground models across land cover classes (Table 9, see LiDAR Accuracy Assessments, page 27).

Table 9: Land Cover Types and Descriptions

Land cover type	Land cover code	Example	Description	Accuracy Assessment Type
Tall Grass	TALL_GRASS	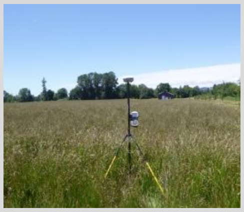	Herbaceous grasslands in advanced stages of growth	VVA
Forest	DEC_FOR, FOREST		Forested areas dominated by deciduous and coniferous species	VVA
Bare Earth	BARE, BE		Areas of bare earth surface	NVA
Urban	URBAN		Areas dominated by urban development, including parks	NVA

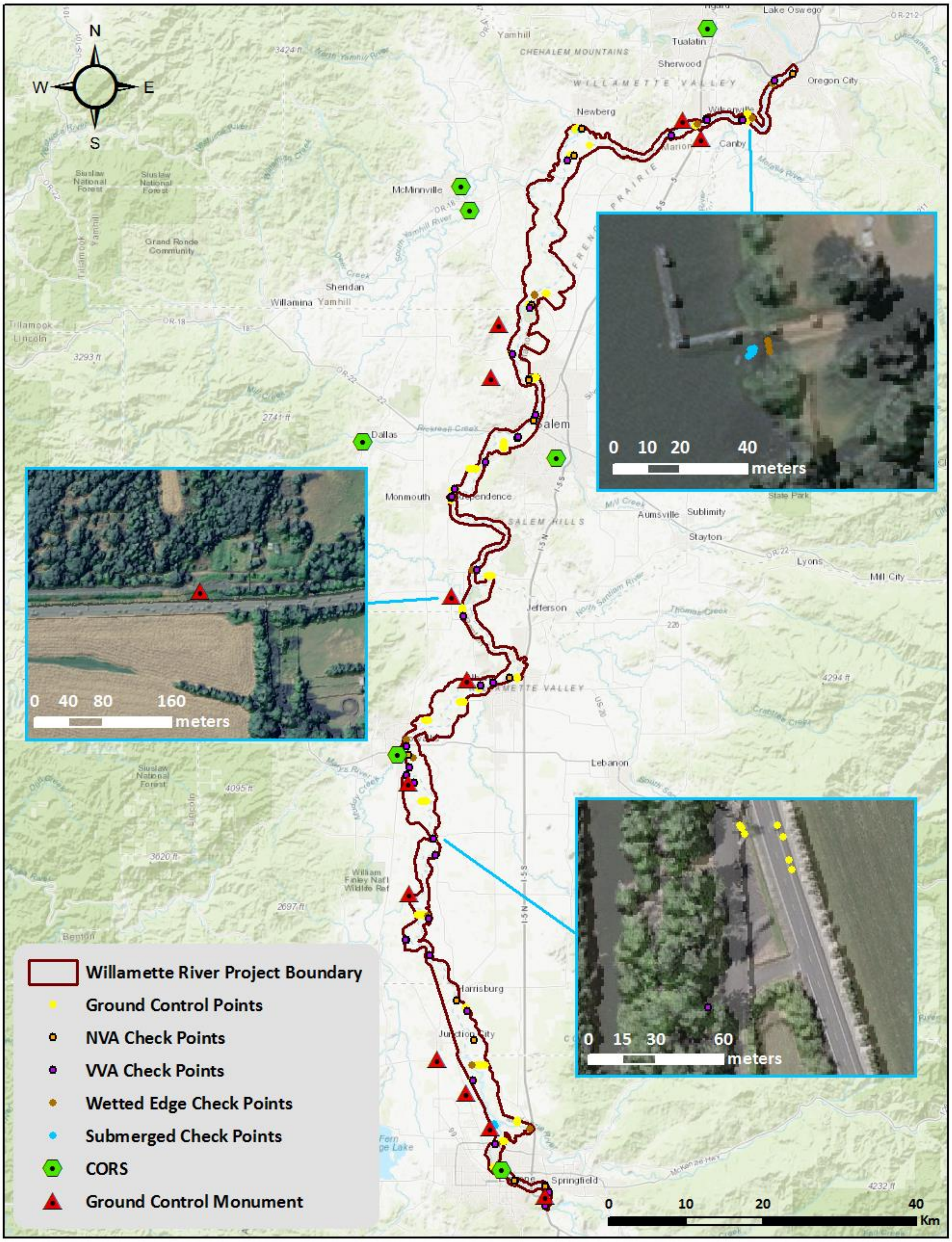

Figure 10: Ground survey location map

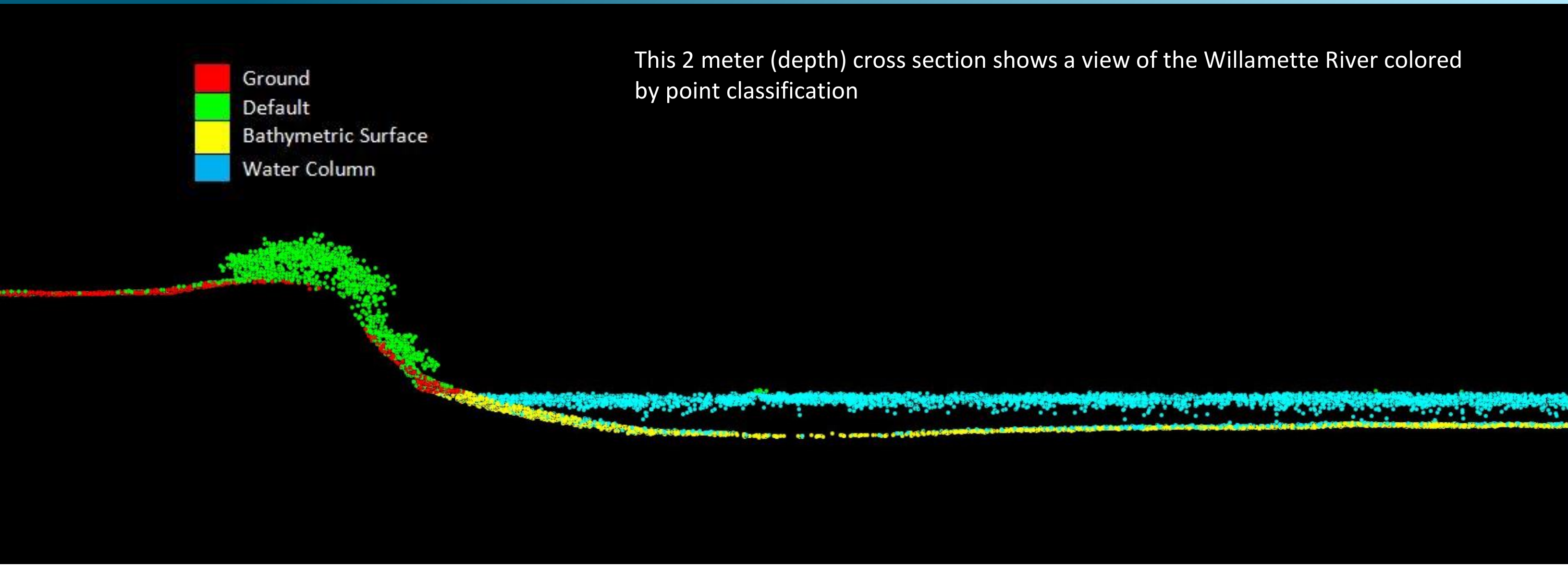

This 2 meter (depth) cross section shows a view of the Willamette River colored by point classification

Topobathymetric LiDAR Data

Upon completion of data acquisition, QSI processing staff initiated a suite of automated and manual techniques to process the data into the requested deliverables. Processing tasks included GPS control computations, smoothed best estimate trajectory (SBET) calculations, kinematic corrections, calculation of laser point position, sensor and data calibration for optimal relative and absolute accuracy, and LiDAR point classification (Table 10).

Riegl's RiProcess software was used to facilitate bathymetric return processing. Once bathymetric points were differentiated, they were spatially corrected for refraction through the water column based on the angle of incidence of the laser. QSI refracted water column points using QSI's proprietary LAS processing software, LAS Monkey. Bathymetric bit flags were applied to all points in which a refraction correction was applied. The resulting point cloud data were classified using both manual and automated techniques. Processing methodologies were tailored for the landscape. Brief descriptions of these tasks are shown in Table 10.

Table 10: ASPRS LAS classification standards applied to the Willamette River Topobathymetric LiDAR dataset

Classification Number	Classification Name	Classification Description
1	Default/Unclassified	Laser returns that are not included in the ground class, composed of vegetation and anthropogenic features
2	Ground	Laser returns that are determined to be ground using automated and manual cleaning algorithms
7	Noise	Laser returns that are often associated with birds, scattering from reflective surfaces, or artificial points below the ground surface
17	Bridge	Bridge decks
40*	Bathymetric Bottom	Refracted Riegl sensor returns that fall within the water's edge breakline which characterize the submerged topography.
41	Water Surface	Green laser returns that are determined to be water surface points using automated and manual cleaning algorithms.
45*	No Bottom Found	Refracted Riegl sensor returns that are determined to be water using automated and manual cleaning algorithms.

*In accordance to the ASPRS Topobathymetric LiDAR Domain Profile, the "Bathymetry flags" extra-byte for all points within Class 40 (Bathymetric Bottom) and Class 45 (No bottom found) were assigned a value of 1 to indicate a refraction correction was applied. (http://www.asprs.org/wp-content/uploads/2010/12/LAS_Domain_Profile_Description_Topo-Bathy_Lidar.pdf)

Table 11: LiDAR processing workflow

LiDAR Processing Step	Software Used
Resolve kinematic corrections for aircraft position data using kinematic aircraft GPS and static ground GPS data. Develop a smoothed best estimate of trajectory (SBET) file that blends post-processed aircraft position with sensor head position and attitude recorded throughout the survey.	POSPac MMS v.8.0
Calculate laser point position by associating SBET position to each laser point return time, scan angle, intensity, etc. Create raw laser point cloud data for the entire survey in *.las (ASPRS v. 1.4) format. Convert data to orthometric elevations by applying a geoid correction.	RiProcess v1.8.2 TerraMatch v.17
Import raw laser points into manageable blocks to perform manual relative accuracy calibration and filter erroneous points. Classify ground points for individual flight lines.	TerraScan v.17
Using ground classified points per each flight line, test the relative accuracy. Perform automated line-to-line calibrations for system attitude parameters (pitch, roll, heading), mirror flex (scale) and GPS/IMU drift. Calculate calibrations on ground classified points from paired flight lines and apply results to all points in a flight line. Use every flight line for relative accuracy calibration.	TerraMatch v.17 RiProcess v1.8.2
Apply refraction correction to all subsurface returns.	LAS Monkey 2.3 (QSI proprietary software)
Classify resulting data to ground and other client designated ASPRS classifications (Table 10). Assess statistical absolute accuracy via direct comparisons of ground classified points to ground control survey data.	TerraScan v.17 TerraModeler v.17
Generate bare earth models as triangulated surfaces. Generate highest hit models as a surface expression of all classified points. Export all surface models as ESRI GRIDs format at a 1 meter pixel resolution.	TerraScan v.17 TerraModeler v.17 ArcMap v. 10.3.1
Export intensity images as GeoTIFFs at a 0.5 meter pixel resolution.	ArcMap v. 10.3.1 Las Product Creator 2.0 (QSI proprietary software)

Bathymetric Refraction

The water surface model used for refraction is generated using NIR points within the breaklines defining the water's edge. Points are filtered and edited to obtain the most accurate representation of the water surface and are used to create a water surface model TIN. A tin model is preferable to a raster based water surface model to obtain the most accurate angle of incidence during refraction. The refraction processing is done using Las Monkey; QSI's proprietary LiDAR processing tool. After refraction, the points are compared against bathymetric control points to assess accuracy.

LiDAR Derived Products

Because hydrographic laser scanners penetrate the water surface to map submerged topography, this affects how the data should be processed and presented in derived products from the LiDAR point cloud. The following discusses certain derived products that vary from the traditional (NIR) specification and delivery format.

Topobathymetric DEMs

Bathymetric bottom returns can be limited by depth, water clarity, and bottom surface reflectivity. Water clarity and turbidity affect the depth penetration capability of the green wavelength laser with returning laser energy diminishing by scattering throughout the water column. Additionally, the bottom surface must be reflective enough to return remaining laser energy back to the sensor at a detectable level. Although the predicted depth penetration range of the Riegl VQ-880-G sensor is 1.5 Secchi depths on brightly reflective surfaces, it is not unexpected to have no bathymetric bottom returns in turbid or non-reflective areas.

As a result, creating digital elevation models (DEMs) presents a challenge with respect to interpolation of areas with no returns. Traditional DEMs are "unclipped", meaning areas lacking ground returns are interpolated from neighboring ground returns (or breaklines in the case of hydro-flattening), with the assumption that the interpolation is close to reality. In bathymetric modeling, these assumptions are prone to error because a lack of bathymetric returns can indicate a change in elevation that the laser can no longer map due to increased depths. The resulting void areas may suggest greater depths, rather than similar elevations from neighboring bathymetric bottom returns. Therefore, QSI created a water polygon with bathymetric coverage to delineate areas with successfully mapped bathymetry.

Insufficiently mapped areas were identified by triangulating bathymetric bottom points with an edge length maximum of 4.56 meters. This ensured all areas of no returns (> 9 m^2), were identified as data voids. This shapefile was used to control the extent of the delivered clipped topobathymetric model to avoid false triangulation (interpolation from TIN'ing) across areas in the water with no bathymetric returns.

Digital Imagery

As with the topobathymetric LiDAR data, the collected digital photographs went through multiple processing steps to create final orthophoto products. Initially, camera exterior orientation parameters were calculated by linking the time of image capture to the smoothed best estimate of trajectory (SBET). Within Inpho's OrthoMaster, individual orthos were output using the LiDAR derived bare earth surface. Orthos were mosaicked within Inpho's OrthoVista, which performs automated project color balancing and seamline creation. The processing workflow for orthophotos is summarized in Table 12.

Table 12: Orthophoto processing workflow

Orthophoto Processing Step	Software Used
Create exterior orientation file (EO) for each image using SBET, camera boresight and event time stamp information.	POSPac MMS v8.0
Convert raw imagery data into geometrically corrected tiff files.	RiProcess v1.8.3
Create ortho images.	Inpho OrthoMaster v.7.1
Mosaic orthoimagery, blending seams between individual photos and applying automatic color-balancing.	Inpho OrthoVista v7.1

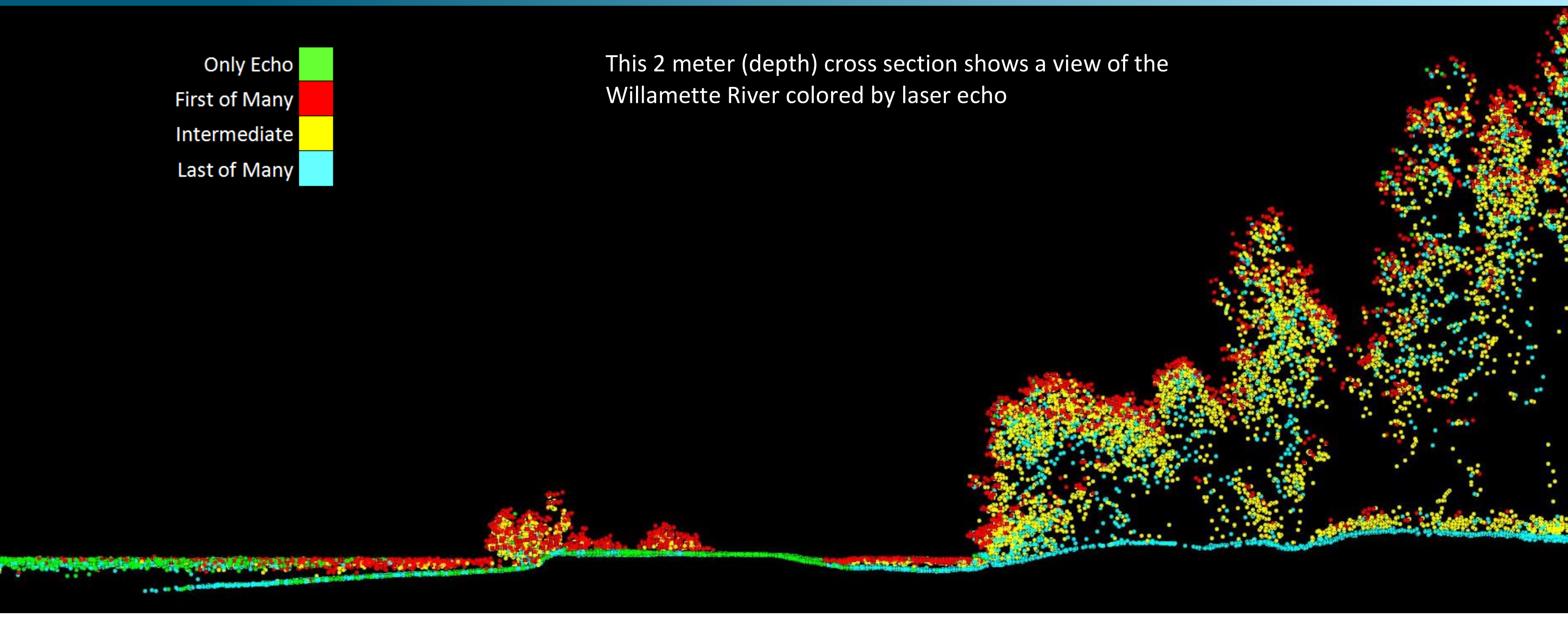

This 2 meter (depth) cross section shows a view of the Willamette River colored by laser echo

LiDAR Point Density

First Return Point Density

The acquisition parameters were designed to acquire an average first-return density of 8 points/m^2. First return density describes the density of pulses emitted from the laser that return at least one echo to the system. Multiple returns from a single pulse were not considered in first return density analysis. Some types of surfaces (e.g., breaks in terrain, water and steep slopes) may have returned fewer pulses than originally emitted by the laser.

First returns typically reflect off the highest feature on the landscape within the footprint of the pulse. In forested or urban areas the highest feature could be a tree, building or power line, while in areas of unobstructed ground, the first return will be the only echo and represents the bare earth surface. The average first-return density of the Willamette River Topobathymetric LiDAR project was 21.23 points/m^2 (Table 13). The statistical and spatial distributions of all first return densities per 100 m x 100 m cell are portrayed in Figure 11 and Figure 12.

Table 13: Average First Return LiDAR point densities

Density Type	Point Density
First Returns	21.23 points/m^2

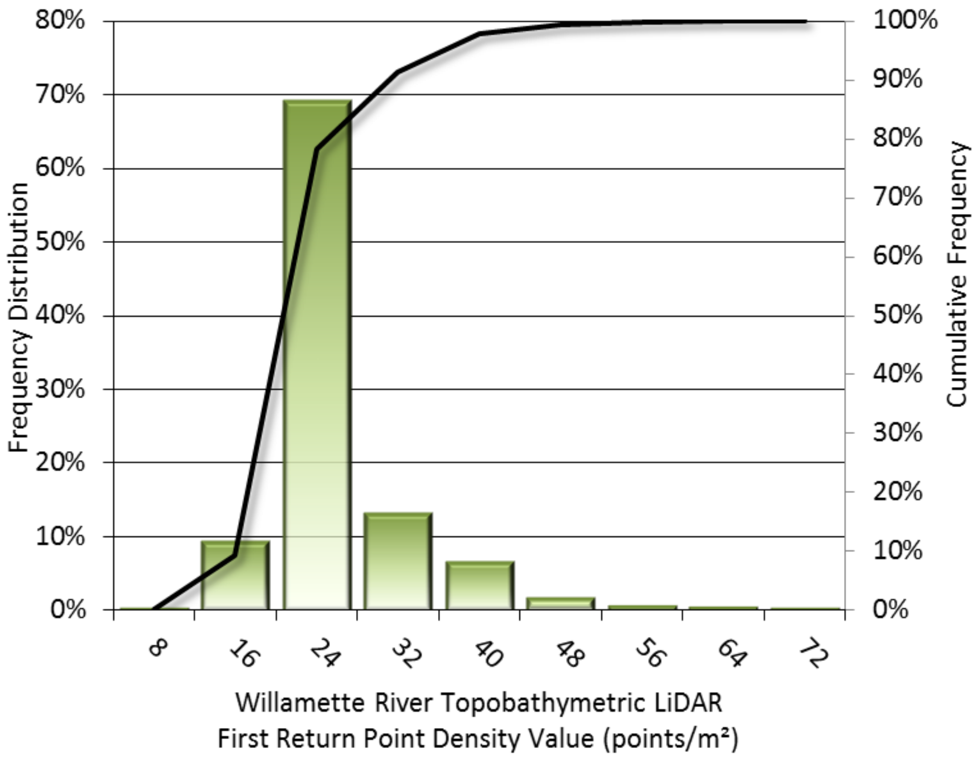

Figure 11: Frequency distribution of first return densities per 100 x 100 m cell

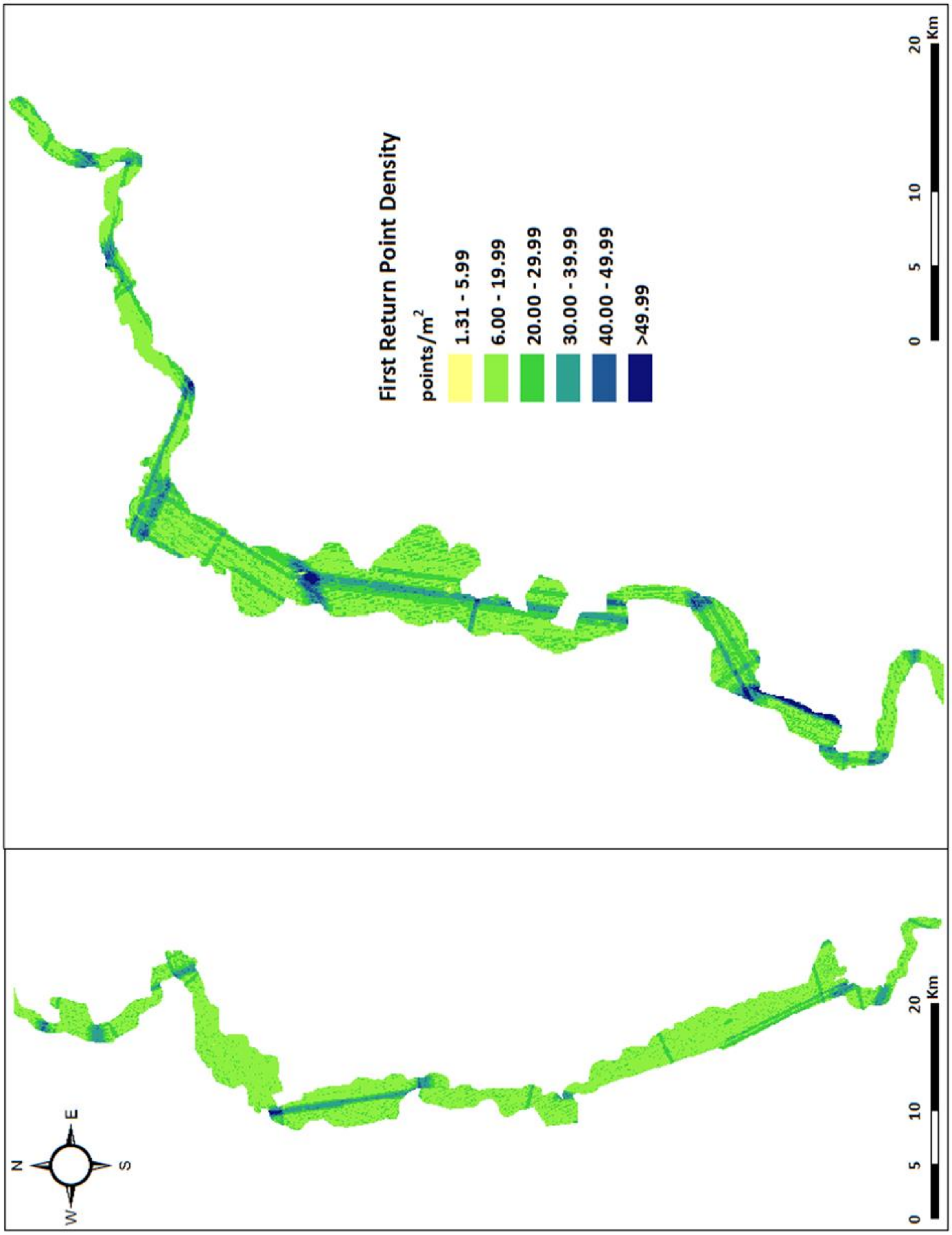

Figure 12: First return density map for the Willamette River Topobathymetric LiDAR site (100 m x 100 m cells)

Bathymetric and Ground Classified Point Densities

The density of ground classified LiDAR returns and bathymetric bottom returns were also analyzed for this project. Terrain character, land cover, and ground surface reflectivity all influenced the density of ground surface returns. In vegetated areas, fewer pulses may have penetrated the canopy, resulting in lower ground density. Similarly, the density of bathymetric bottom returns was influenced by turbidity, depth, and bottom surface reflectivity. In turbid areas, fewer pulses may have penetrated the water surface, resulting in lower bathymetric density.

The ground and bathymetric bottom classified density of LiDAR data for the Willamette River Topobathymetric LiDAR project was 5.69 points/m^2 (Table 14). The statistical and spatial distributions of ground classified and bathymetric bottom return densities per 100 m x 100 m cell are portrayed in Figure 13 and Figure 14.

Additionally, for the Willamette River Topobathymetric LiDAR project, density values of only bathymetric bottom returns were calculated for areas considered successfully mapped. Areas lacking bathymetric returns were not considered in calculating an average density value. Within the successfully mapped area, a bathymetric bottom return density of 7.28 points/m^2 was achieved.

Table 14: Average ground and bathymetric bottom classified LiDAR point densities

Density Type	Point Density
Ground and Bathymetric Bottom Classified Returns	5.69 points/m²
Bathymetric Bottom Classified Returns	7.28 points/m²

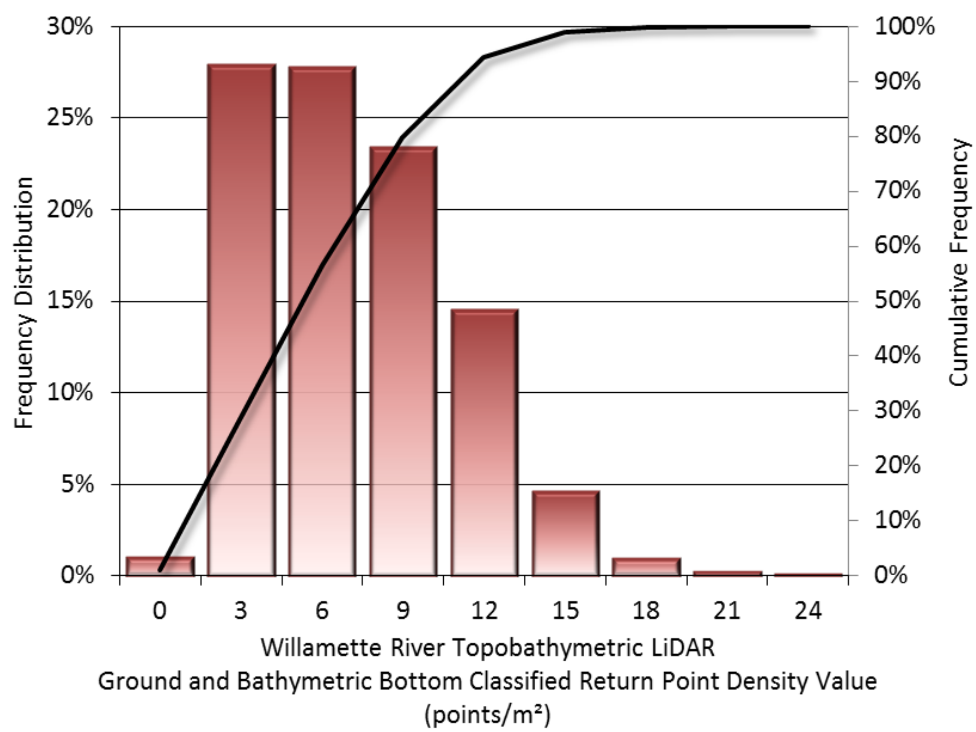

Figure 13: Frequency distribution of ground and bathymetric bottom classified return densities per 100 x 100 m cell

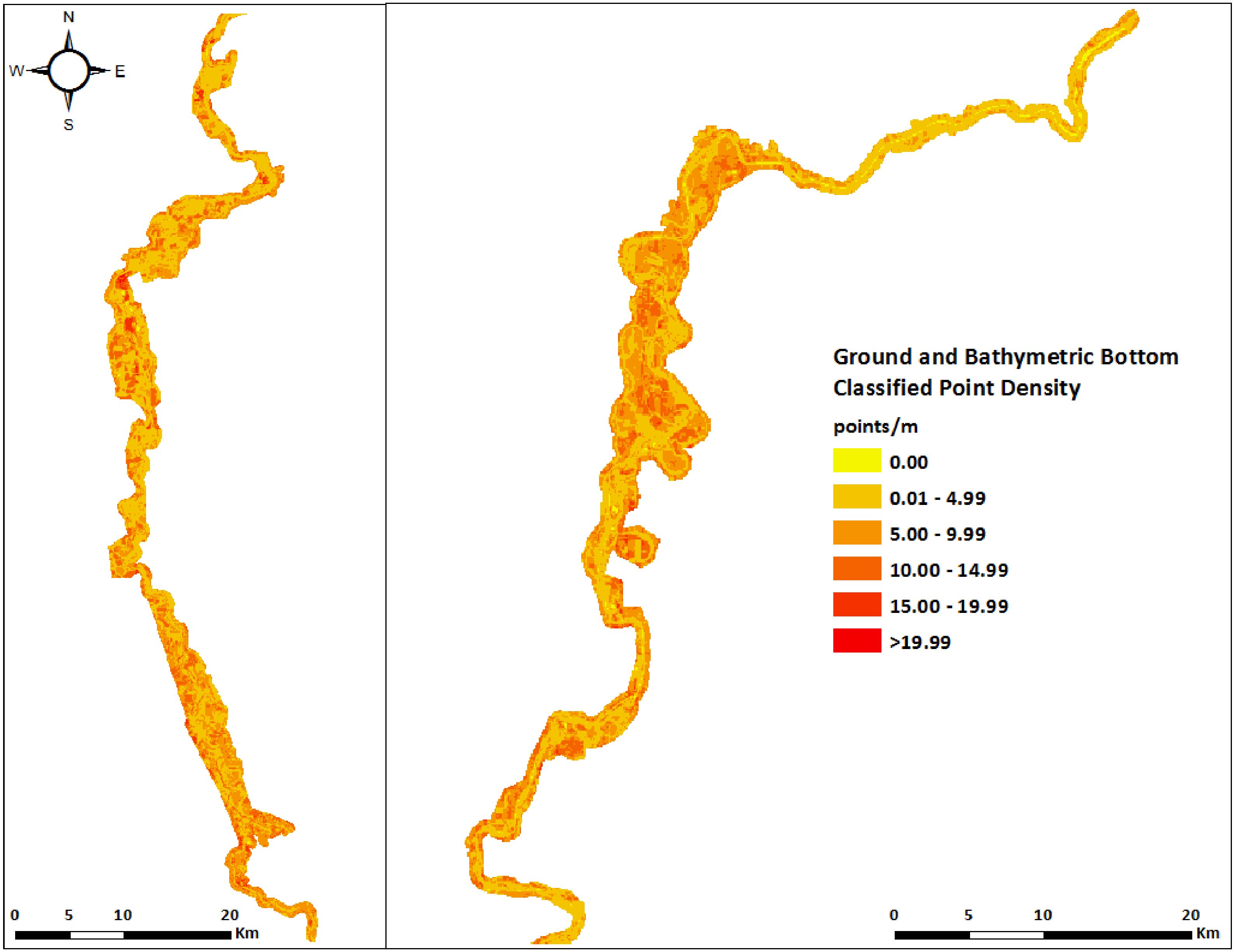

Figure 14: Ground and bathymetric bottom classified density map for the Willamette River Topobathymetric LiDAR site (100 m x 100 m cells)

LiDAR Accuracy Assessments

The accuracy of the LiDAR data collection can be described in terms of absolute accuracy (the consistency of the data with external data sources) and relative accuracy (the consistency of the dataset with itself). See Appendix A for further information on sources of error and operational measures used to improve relative accuracy.

LiDAR Absolute Accuracy

Absolute accuracy was assessed using Non-vegetated Vertical Accuracy (NVA) reporting designed to meet guidelines presented in the FGDC National Standard for Spatial Data Accuracy[4]. NVA compares known ground check point data collected on open, bare earth surfaces with level slope (<20°) to the triangulated surface generated by the LiDAR points. NVA is a measure of the accuracy of LiDAR point data in open areas where the LiDAR system has a high probability of measuring the ground surface and is evaluated at the 95% confidence interval (1.96 * $RMSE_Z$), as shown in Table 15.

The mean and standard deviation (sigma σ) of divergence of the ground surface model from ground check point coordinates are also considered during accuracy assessment. These statistics assume the error for x, y and z is normally distributed, and therefore the skew and kurtosis of distributions are also considered when evaluating error statistics. For the Willamette River Topobathymetric LiDAR survey, 20 ground check points were taken resulting in a non-vegetated vertical accuracy of 0.047 meters compared to the bare earth DEM and 0.055 meters compared to the unclassified LAS, with 95% confidence (Figure 15).

QSI also assessed absolute accuracy using 2,493 ground control points. Although these points were used in the calibration and post-processing of the LiDAR point cloud, they still provide a good indication of the overall accuracy of the LiDAR dataset, and therefore have been provided in Table 15 and Figure 17.

Table 15: Topographic Absolute Accuracy Results

Absolute Accuracy			
	Ground Check Points (NVA), as compared to the Bare Earth DEM	Ground Check Points (NVA), as compared to the Unclassified LAS	Ground Control Points
Sample	20 points	20 points	2,493 points
NVA (1.96*$RMSE_Z$)	0.047 m	0.055 m	0.048 m
Average	-0.010 m	-0.011 m	-0.009 m
Median	-0.006 m	-0.011 m	-0.009 m
$RMSE_Z$	0.024 m	0.028 m	0.025 m
Standard Deviation (1σ)	0.023 m	0.027 m	0.023 m

[4] Federal Geographic Data Committee, ASPRS POSITIONAL ACCURACY STANDARDS FOR DIGITAL GEOSPATIAL DATA EDITION 1, Version 1.0, NOVEMBER 2014. http://www.asprs.org/PAD-Division/ASPRS-POSITIONAL-ACCURACY-STANDARDS-FOR-DIGITAL-GEOSPATIAL-DATA.html.

Additionally, topobathymetric check points were collected in order to assess vertical accuracies of the topobathymetric surface in and around the river. These check points were collected along the water's edge and along the river bottom for evaluation against the topobathymetric ground surface. The wetted edge check points yielded a $RMSE_Z$ vertical accuracy of 0.029 meters and the submerged topobathymetric check points yielded a $RMSE_Z$ vertical accuracy of 0.036 meters (Table 16).

Table 16: Bathymetric Absolute Accuracy Results

Absolute Accuracy		
	Wetted Edge Check Points	**Submerged Bathymetric Check Points**
Sample	126 Points	484 Points
Average	0.000 m	-0.008 m
Median	0.003 m	-0.006 m
$RMSE_Z$	0.029 m	0.036 m
Standard Deviation (1σ)	0.029 m	0.035 m
1.96*RMSE	0.057 m	0.070 m

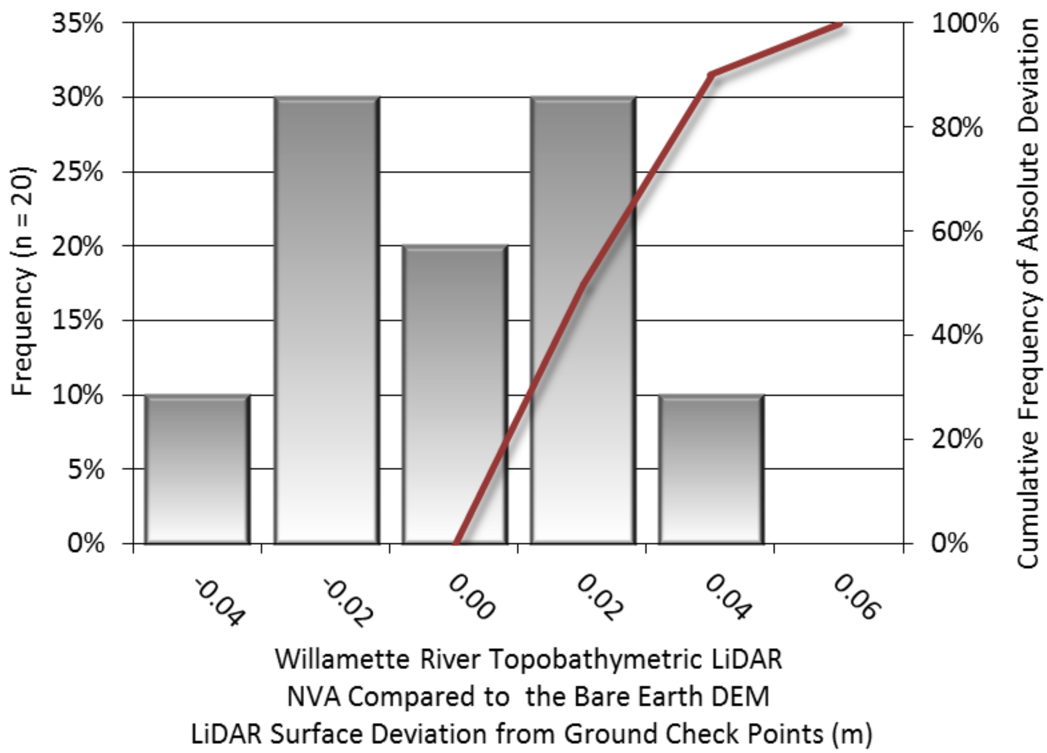

Figure 15: Frequency histogram for LiDAR surface deviation from ground check point values

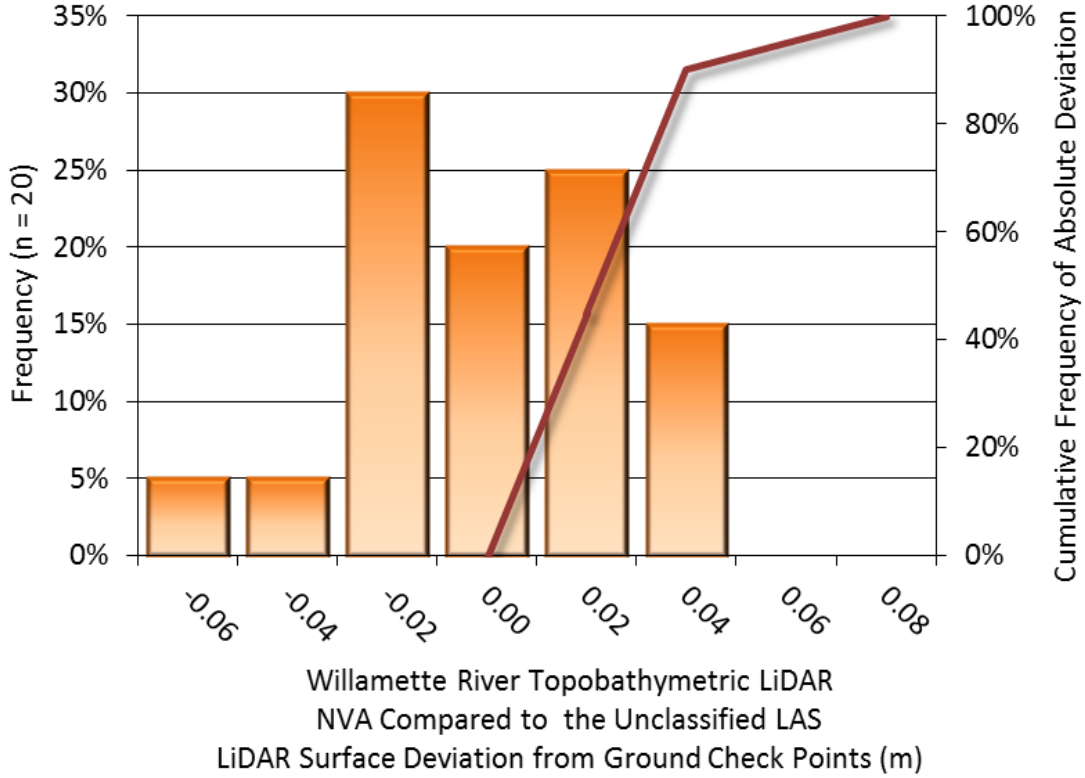

Figure 16: Frequency histogram for LiDAR surface deviation from ground check point values

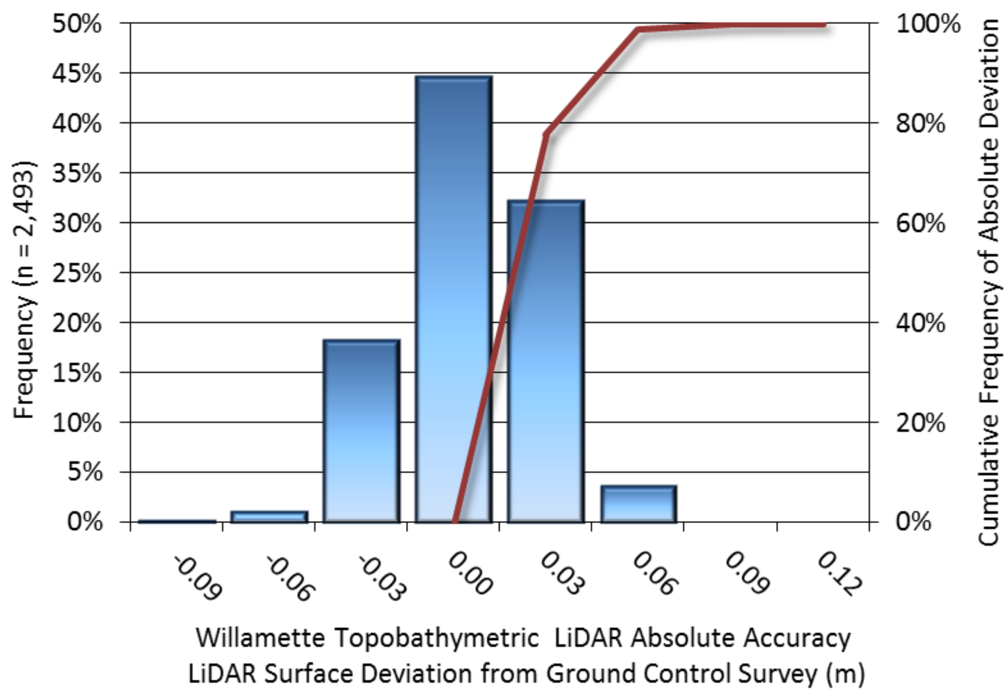

Figure 17: Frequency histogram for LiDAR surface deviation from ground control point values

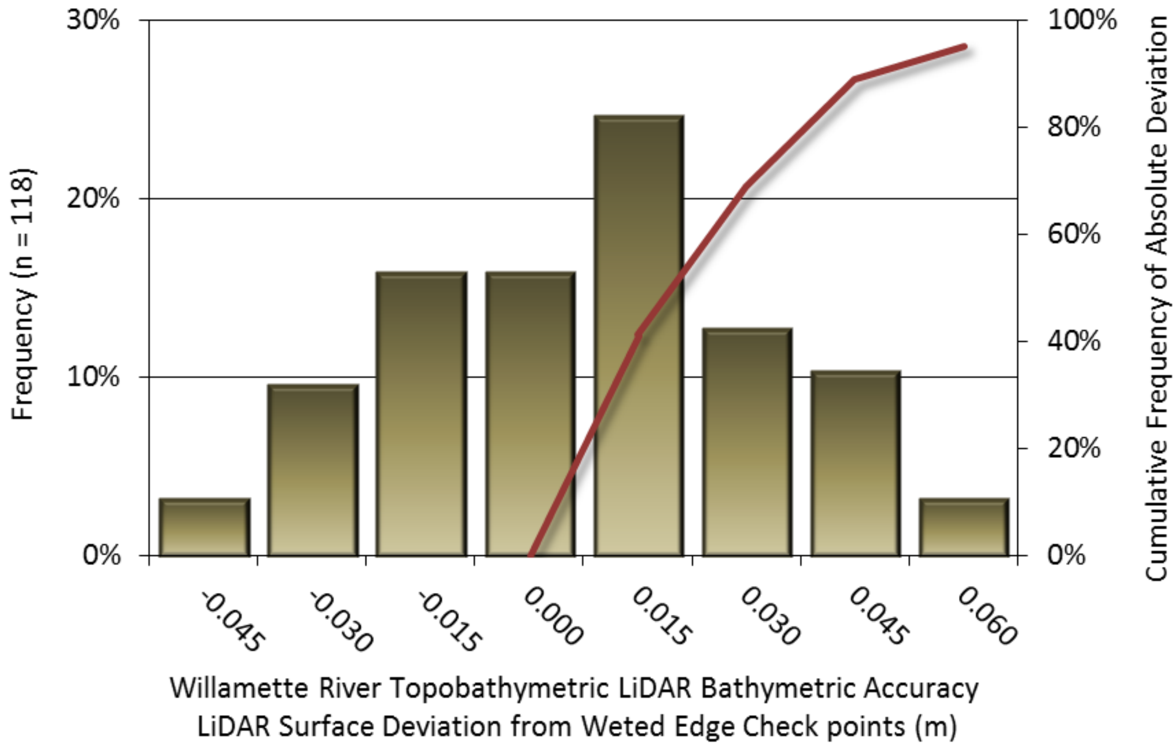

Figure 18: Frequency histogram for LiDAR surface deviation wetted edge check point values

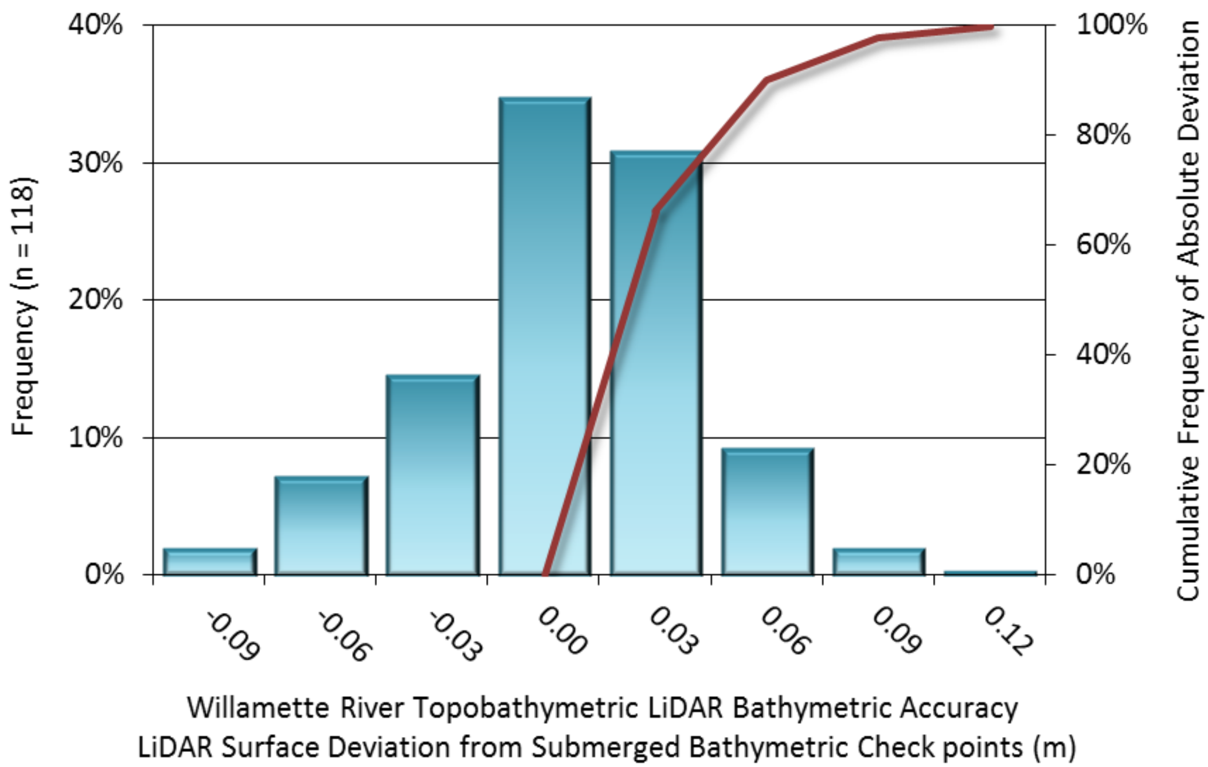

Figure 19: Frequency histogram for LiDAR surface deviation bathymetric check point values

LiDAR Vegetated Vertical Accuracies

QSI also assessed vertical accuracy using Vegetated Vertical Accuracy (VVA) reporting. VVA compares known ground check point data collected over vegetated surfaces using land class descriptions to the triangulated ground surface generated by the ground classified LiDAR points. VVA is evaluated at the 95th percentile (Table 17, Figure 20).

VVA for the first delivery of Willamette River Topobathymetric LiDAR project was computed to be 29.5 cm, exceeding the maximum allowable VVA of 14.7 cm for Quality Level 0 (QL0). However, the necessary acquisition time frame for collecting the best bathymetric LiDAR data took place during the spring season when terrestrial vegetation within some portions of the area of interest was especially dense.

Therefore, in accordance with ASPRS recommendations, low confidence polygons based on ground density have been created to delineate where the elevation data may be less reliable due to lack of laser penetration through dense vegetation. VVA statistics excluding outlier check points greater than 3 standard deviations were computed, resulting in an alternative VVA of 18.1cm, as shown in Table 17.

Table 17: Vegetated Vertical Accuracy for the Willamette River Topobathymetric LiDAR Project

	VVA Check Points	VVA Check Points, Outliers Excluded
Sample	40 points	37 points
Average Dz	0.088 m	0.070 m
Median	0.069 m	0.062 m
$RMSE_Z$	0.125 m	0.093 m
Standard Deviation (1σ)	0.083 m	0.063 m
95^{th} Percentile	0.295 m	0.181 m

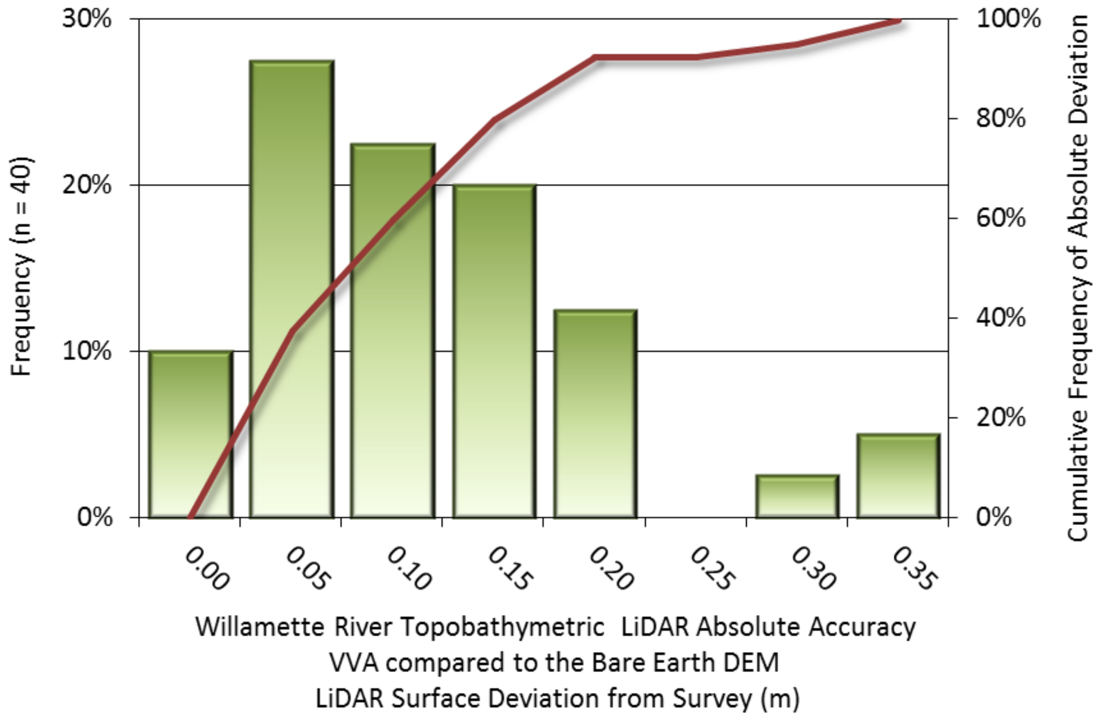

Figure 20: Frequency histogram for LiDAR surface deviation from all land cover class point values (VVA)

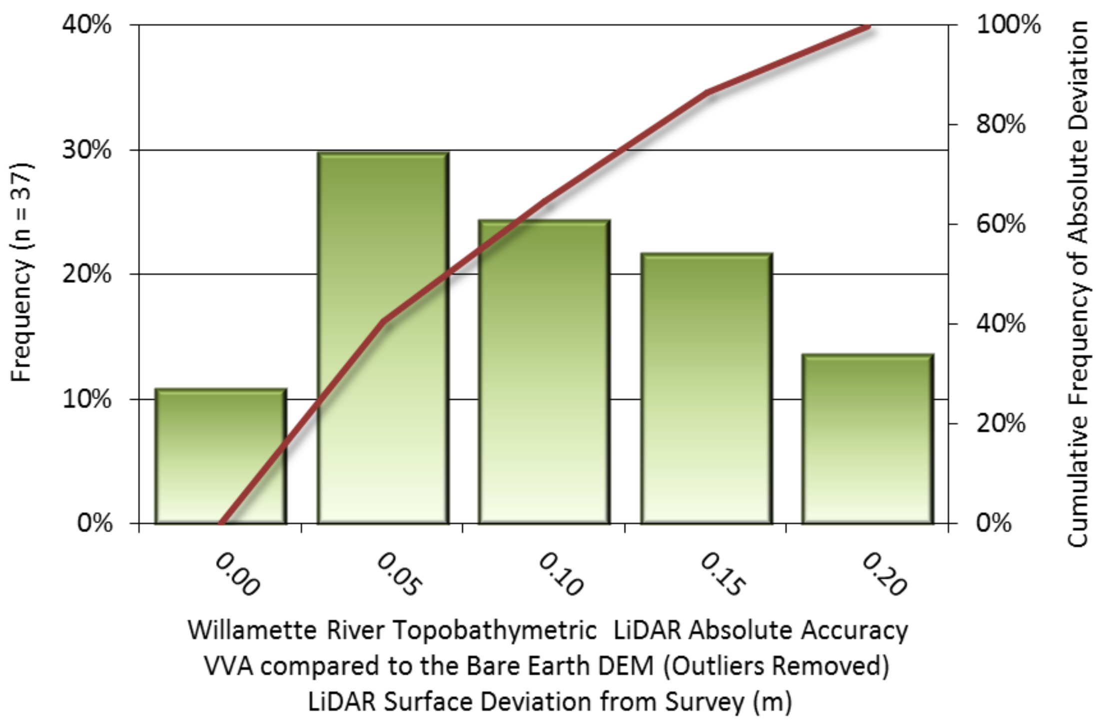

Figure 21: Frequency histogram for LiDAR surface deviation from all land cover class point values with outlier points removed (VVA)

LiDAR Relative Vertical Accuracy

Relative vertical accuracy refers to the internal consistency of the data set as a whole: the ability to place an object in the same location given multiple flight lines, GPS conditions, and aircraft attitudes. When the LiDAR system is well calibrated, the swath-to-swath vertical divergence is low (<0.10 meters). The relative vertical accuracy was computed by comparing the ground surface model of each individual flight line with its neighbors in overlapping regions. The average (mean) line to line relative vertical accuracy for the Willamette River, Oregon LiDAR project was 0.024 meters (Table 18, Figure 22).

Table 18: Relative accuracy results

Relative Accuracy	
Sample	570 surfaces
Average	0.024 m
Median	0.023 m
RMSE	0.025 m
Standard Deviation (1σ)	0.006 m
1.96σ	0.012 m

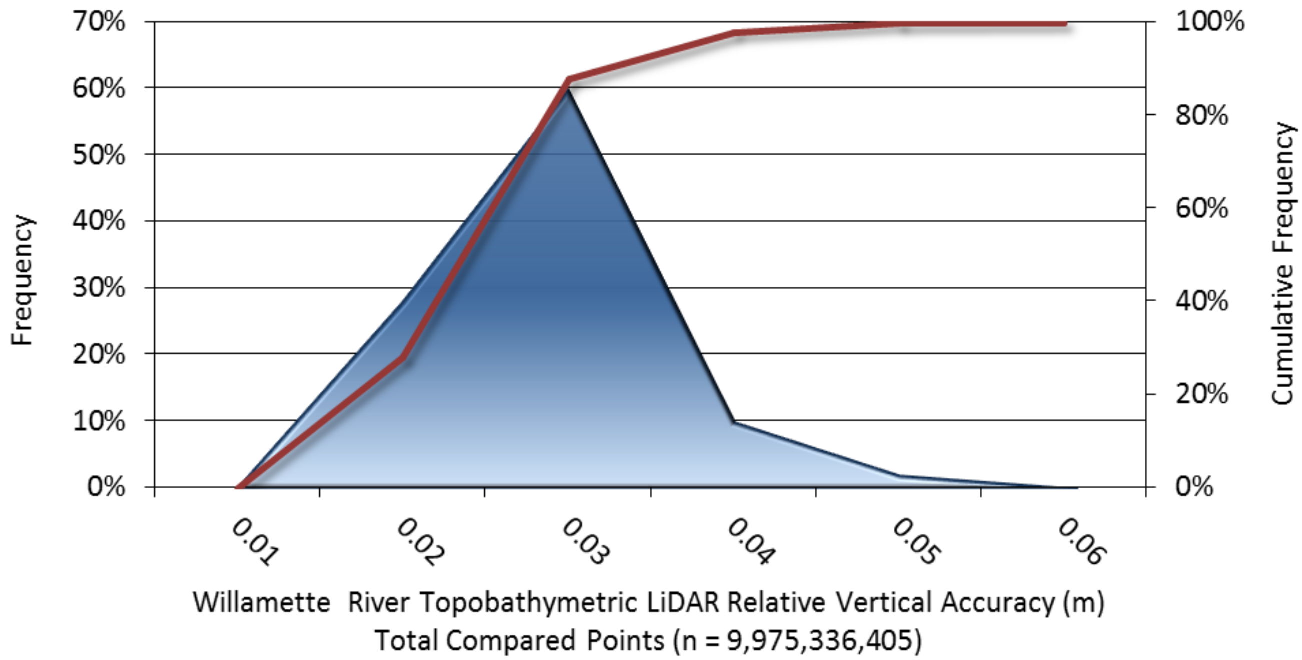

Figure 22: Frequency plot for relative vertical accuracy between flight lines

Digital Imagery Accuracy Assessment

An independent accuracy assessment for the aerial imagery was not performed as images were directly georeferenced and no ground control air targets were collected for the project. It is, however, reasonable to assume similar accuracy results as were achieved by the boresight flight. Table 19 shows the root mean square for the boresight aerial triangulation adjustment to ground control points extracted from LiDAR collected during the boresight flight.

Table 19: RMS of ground control residuals from the camera boresight

Ground Control RMSE for Boresight Mission	
$RMSE_X$	0.03 m
$RMSE_Y$	0.32 m
$RMSE_Z$	0.22 m

Figure 23: Image displaying the co-registration between the LiDAR intensity image and the orthophoto at a location within the Willamette River Topobathymetric LiDAR site.

Certifications

Quantum Spatial, Inc. provided LiDAR services for the Willamette River Topobathymetric LiDAR project as described in this report.

I, Tucker Selko, have reviewed the attached report for completeness and hereby state that it is a complete and accurate report of this project.

Tucker Selko (Dec 14, 2017)

Dec 14, 2017

Tucker Selko
Project Manager
Quantum Spatial, Inc.

I, Evon P. Silvia, PLS, being duly registered as a Professional Land Surveyor in and by the state of Oregon, hereby certify that the methodologies, static GNSS occupations used during airborne flights, and ground survey point collection were performed using commonly accepted Standard Practices. Field work conducted for this report was conducted between May 24 and June 23, 2017.

Accuracy statistics shown in the Accuracy Section of this Report have been reviewed by me and found to meet the “National Standard for Spatial Data Accuracy”.

Dec 14, 2017

Evon P. Silvia, PLS
Quantum Spatial, Inc.
Corvallis, OR 97333

REGISTERED
PROFESSIONAL
LAND SURVEYOR

OREGON
JUNE 10, 2014
EVON P. SILVIA
81104LS

EXPIRES: 06/30/2018

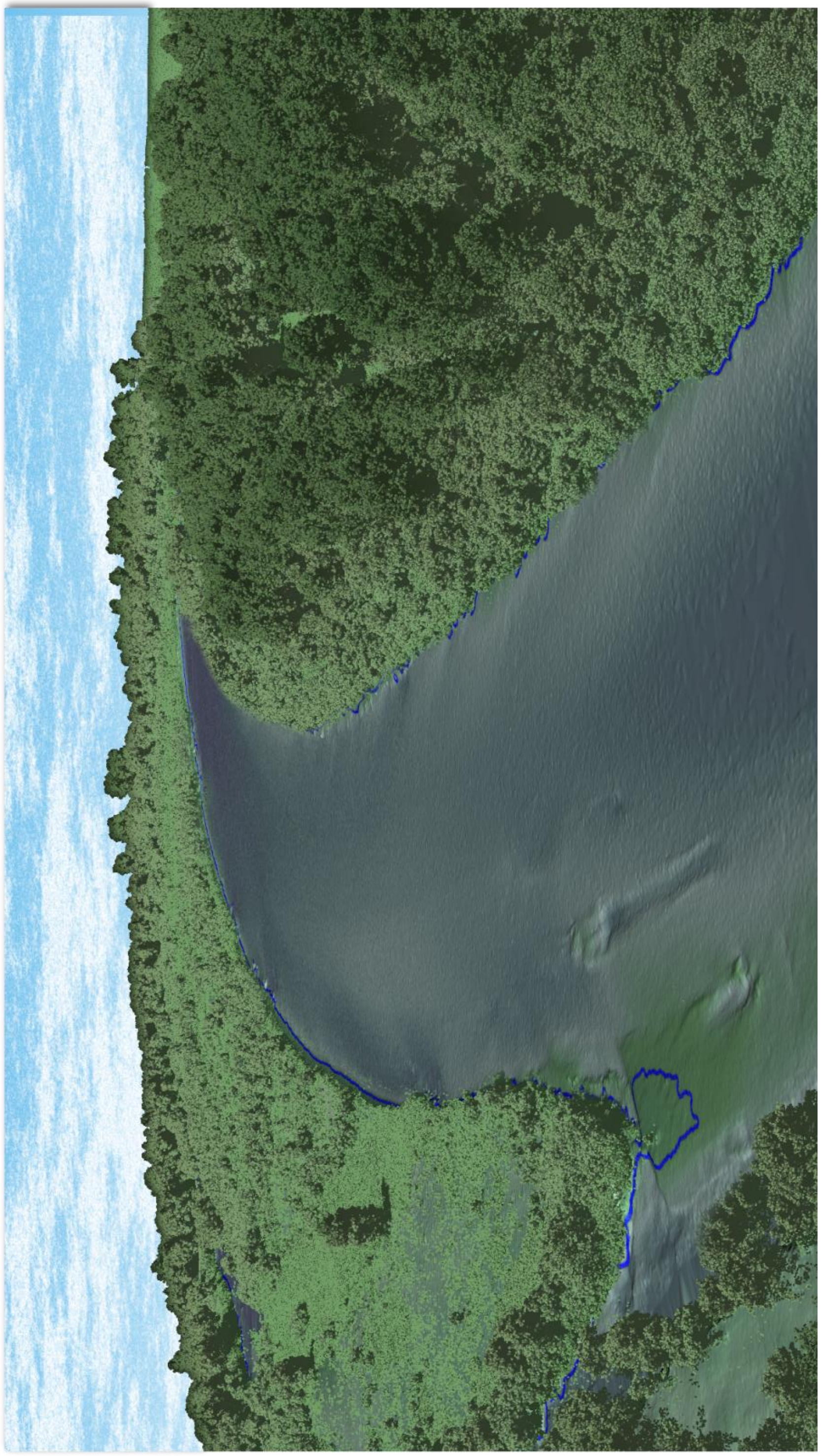

Figure 24: View looking north over the Willamette River Topobathymetric LiDAR project area. The image was created from the LiDAR bare earth model overlaid with the above-ground point cloud, colored by elevation.

Figure 25: View looking southeast over Willamette River Topobathymetric LiDAR. The image was created from the LiDAR bare earth model overlaid with the above-ground point cloud, colored by elevation.

GLOSSARY

1-sigma (σ) Absolute Deviation: Value for which the data are within one standard deviation (approximately 68th percentile) of a normally distributed data set.

1.96 * RMSE Absolute Deviation: Value for which the data are within two standard deviations (approximately 95th percentile) of a normally distributed data set, based on the FGDC standards for Non-vegetated Vertical Accuracy (FVA) reporting.

Accuracy: The statistical comparison between known (surveyed) points and laser points. Typically measured as the standard deviation (sigma σ) and root mean square error (RMSE).

> **Absolute Accuracy:** The vertical accuracy of LiDAR data is described as the mean and standard deviation (sigma σ) of divergence of LiDAR point coordinates from ground survey point coordinates. To provide a sense of the model predictive power of the dataset, the root mean square error (RMSE) for vertical accuracy is also provided. These statistics assume the error distributions for x, y and z are normally distributed, and thus we also consider the skew and kurtosis of distributions when evaluating error statistics.
>
> **Relative Accuracy:** Relative accuracy refers to the internal consistency of the data set; i.e., the ability to place a laser point in the same location over multiple flight lines, GPS conditions and aircraft attitudes. Affected by system attitude offsets, scale and GPS/IMU drift, internal consistency is measured as the divergence between points from different flight lines within an overlapping area. Divergence is most apparent when flight lines are opposing. When the LiDAR system is well calibrated, the line-to-line divergence is low (<10 cm).
>
> **Root Mean Square Error (RMSE):** A statistic used to approximate the difference between real-world points and the LiDAR points. It is calculated by squaring all the values, then taking the average of the squares and taking the square root of the average.

Data Density: A common measure of LiDAR resolution, measured as points per square meter.

Digital Elevation Model (DEM): File or database made from surveyed points, containing elevation points over a contiguous area. Digital terrain models (DTM) and digital surface models (DSM) are types of DEMs. DTMs consist solely of the bare earth surface (ground points), while DSMs include information about all surfaces, including vegetation and man-made structures.

Intensity Values: The peak power ratio of the laser return to the emitted laser, calculated as a function of surface reflectivity.

Nadir: A single point or locus of points on the surface of the earth directly below a sensor as it progresses along its flight line.

Overlap: The area shared between flight lines, typically measured in percent. 100% overlap is essential to ensure complete coverage and reduce laser shadows.

Pulse Rate (PR): The rate at which laser pulses are emitted from the sensor; typically measured in thousands of pulses per second (kHz).

Pulse Returns: For every laser pulse emitted, the number of wave forms (i.e., echoes) reflected back to the sensor. Portions of the wave form that return first are the highest element in multi-tiered surfaces such as vegetation. Portions of the wave form that return last are the lowest element in multi-tiered surfaces.

Real-Time Kinematic (RTK) Survey: A type of surveying conducted with a GPS base station deployed over a known monument with a radio connection to a GPS rover. Both the base station and rover receive differential GPS data and the baseline correction is solved between the two. This type of ground survey is accurate to 1.5 cm or less.

Post-Processed Kinematic (PPK) Survey: GPS surveying is conducted with a GPS rover collecting concurrently with a GPS base station set up over a known monument. Differential corrections and precisions for the GNSS baselines are computed and applied after the fact during processing. This type of ground survey is accurate to 1.5 cm or less.

Scan Angle: The angle from nadir to the edge of the scan, measured in degrees. Laser point accuracy typically decreases as scan angles increase.

Native LiDAR Density: The number of pulses emitted by the LiDAR system, commonly expressed as pulses per square meter.

Appendix A - Accuracy Controls

Relative Accuracy Calibration Methodology:

Manual System Calibration: Calibration procedures for each mission require solving geometric relationships that relate measured swath-to-swath deviations to misalignments of system attitude parameters. Corrected scale, pitch, roll and heading offsets were calculated and applied to resolve misalignments. The raw divergence between lines was computed after the manual calibration was completed and reported for each survey area.

Automated Attitude Calibration: All data were tested and calibrated using TerraMatch automated sampling routines. Ground points were classified for each individual flight line and used for line-to-line testing. System misalignment offsets (pitch, roll and heading) and scale were solved for each individual mission and applied to respective mission datasets. The data from each mission were then blended when imported together to form the entire area of interest.

Automated Z Calibration: Ground points per line were used to calculate the vertical divergence between lines caused by vertical GPS drift. Automated Z calibration was the final step employed for relative accuracy calibration.

LiDAR accuracy error sources and solutions:

Type of Error	Source	Post Processing Solution
GPS (Static/Kinematic)	Long Base Lines	None
	Poor Satellite Constellation	None
	Poor Antenna Visibility	Reduce Visibility Mask
Relative Accuracy	Poor System Calibration	Recalibrate IMU and sensor offsets/settings
	Inaccurate System	None
Laser Noise	Poor Laser Timing	None
	Poor Laser Reception	None
	Poor Laser Power	None
	Irregular Laser Shape	None

Operational measures taken to improve relative accuracy:

Low Flight Altitude: Terrain following was employed to maintain a constant above ground level (AGL). Laser horizontal errors are a function of flight altitude above ground (about 1/3000th AGL flight altitude).

Focus Laser Power at narrow beam footprint: A laser return must be received by the system above a power threshold to accurately record a measurement. The strength of the laser return (i.e., intensity) is a function of laser emission power, laser footprint, flight altitude and the reflectivity of the target. While surface reflectivity cannot be controlled, laser power can be increased and low flight altitudes can be maintained.

Reduced Scan Angle: Edge-of-scan data can become inaccurate. The scan angle was reduced to a maximum of ±20^{o} from nadir, creating a narrow swath width and greatly reducing laser shadows from trees and buildings.

Quality GPS: Flights took place during optimal GPS conditions (e.g., 6 or more satellites and PDOP [Position Dilution of Precision] less than 3.0). Before each flight, the PDOP was determined for the survey day. During all flight times, a dual frequency DGPS base station recording at 1 second epochs was utilized and a maximum baseline length between the aircraft and the control points was less than 13 nm at all times.

Ground Survey: Ground survey point accuracy (<1.5 cm RMSE) occurs during optimal PDOP ranges and targets a minimal baseline distance of 4 miles between GPS rover and base. Robust statistics are, in part, a function of sample size (n) and distribution. Ground survey points are distributed to the extent possible throughout multiple flight lines and across the survey area.

50% Side-Lap (100% Overlap): Overlapping areas are optimized for relative accuracy testing. Laser shadowing is minimized to help increase target acquisition from multiple scan angles. Ideally, with a 50% side-lap, the nadir portion of one flight line coincides with the swath edge portion of overlapping flight lines. A minimum of 50% side-lap with terrain-followed acquisition prevents data gaps.

Opposing Flight Lines: All overlapping flight lines have opposing directions. Pitch, roll and heading errors are amplified by a factor of two relative to the adjacent flight line(s), making misalignments easier to detect and resolve.